catalysts

MDPI

Supplementary Materials

Photochemical Study of a New Bimolecular Photoinitiating System for Vat Photopolymerization 3D Printing Techniques under Visible Light

Paweł Fiedor [1], Maciej Pilch[1], Patryk Szymaszek[1], Anna Chachaj-Brekiesz [2], Mariusz Galek[3] and Joanna Ortyl [1,3]*

[1] Cracow University of Technology, Faculty of Chemical Engineering and Technology, Warszawska 24, 31-155 Cracow, Poland
[2] Jagiellonian University, Faculty of Chemistry, Gronostajowa 2, 30-387 Cracow, Poland
[3] Photo HiTech Ltd., Bobrzyńskiego 14, 30-348 Cracow, Poland

* Correspondence: jortyl@chemia.pk.edu.pl

Received: date; Accepted: date; Published: date

Synthesis - Chemicals and general synthetic procedures of 2-amino-4,6-diphenylpyridine-3-carbonitrile derivatives

Structural formulas of 2-amino-4,6-diphenyl-pyridine-3-carbonitrile derivatives S1-S8 which were synthesized following modified procedure [1, 2] were presented in Table S.1.

All inorganic salts organic reagents, and solvents were analytically pure and used as received. Structure and purity of obtained products were confirmed by NMR and LC–MS analysis. ^{1}H and ^{13}CNMR spectra were recorded in DMSO–D_6 on Avance III HD 400 MHz (Bruker) spectrometer. Chemical shifts were reported in parts per million (δ) and referenced to residual protonated solvent peak (δ=2.50 ppm in ^{1}HNMR spectra and 39.52 ppm ^{13}CNMR spectra). LC–MS analyses were obtained on LCMS–2020 (Shimadzu) with ESI ionization method. Melting points were determined with capillary melting–point apparatus and were uncorrected.

Table 1. Structures of investigated molecular fluorescent sensors for photopolymerization processes

Structures of the derivatives of 2-amino-4,6-diphenyl-pyridine-3-carbonitrile		
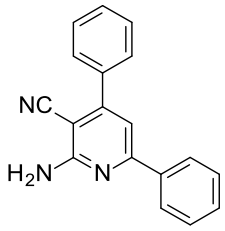	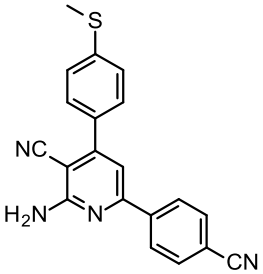	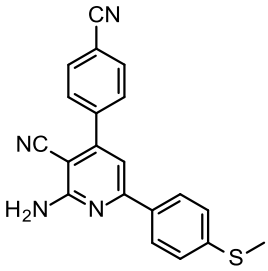
S1	S2	S3
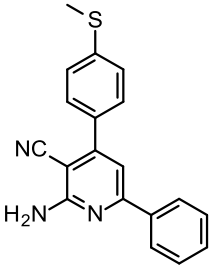	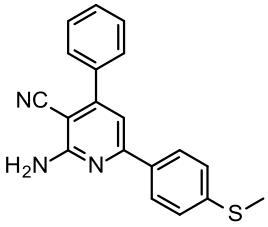	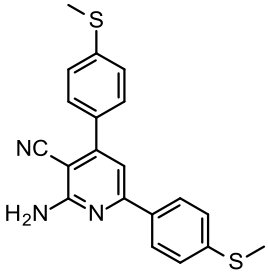
S4	S5	S6
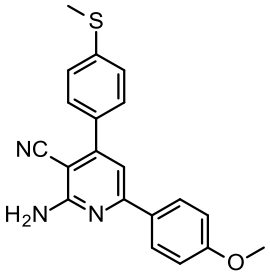		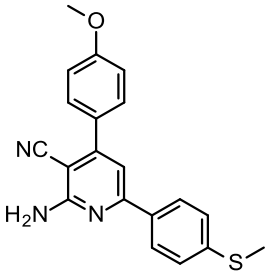
S7		S8

2-amino-4,6-diphenylpyridine-3-carbonitrile [1], ***S1***

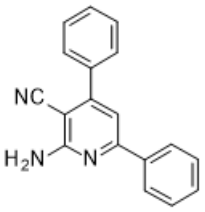

Yield: 0.698 g (33%); m.p. 185 °C; ^{1}H NMR (400 MHz, DMSO) δ 8.17 – 8.10 (m, 2H), 7.72 – 7.65 (m, 2H), 7.60 – 7.53 (m, 3H), 7.52 – 7.46 (m, 3H), 7.28 (s, 1H), 7.02 (brs, 2H); ^{13}C NMR (101 MHz, DMSO) δ 160.86, 158.61, 154.89, 137.54, 136.99, 130.09, 129.58, 128.72, 128.62, 128.33, 127.24, 117.03, 109.24, 86.64; MS (ESI) m/z(%): 272 ([M+H]$^{+}$, 100%); purity (LC): >99%.

2-amino-6-(4-cyanophenyl)-4-(4-methylsulfanylphenyl)pyridine-3-carbonitrile, ***S2***

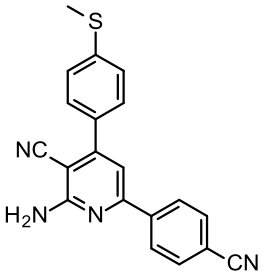

Yield: 0.508 g (23%); m.p. 256 °C; ^{1}H NMR (400 MHz, DMSO) δ 8.34 – 8.28 (m, 2H), 8.00 – 7.94 (m, 2H), 7.68 – 7.62 (m, 2H), 7.45 – 7.41 (m, 2H), 7.39 (s, 1H), 7.13 (s, 2H), 2.55 (s, 3H); ^{13}C NMR (101 MHz, DMSO) δ 160.85, 156.46, 154.66, 141.76, 140.90, 132.73, 132.58, 128.88, 127.95, 125.54, 118.65, 116.85, 112.24, 109.77, 87.56, 14.29; MS (ESI) m/z(%): 343 ([M+H]$^{+}$, 100%); purity (LC): >96%.

2-amino-4-(4-cyanophenyl)-6-(4-methylsulfanylphenyl)pyridine-3-carbonitrile, ***S3***

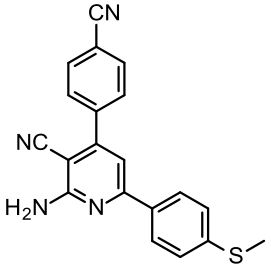

Yield: 0.737 g (33%); m.p. 195 °C; ^{1}H NMR (400 MHz, DMSO) δ 8.13 – 8.07 (m, 2H), 8.06 – 8.02 (m, 2H), 7.89 – 7.84 (m, 2H), 7.38 – 7.32 (m, 2H), 7.31 (s, 1H), 7.11 (s, 2H), 2.53 (s, 3H); ^{13}C NMR (101 MHz, DMSO) δ 160.69, 158.29, 153.08, 141.55, 141.47, 133.52, 132.60, 129.47, 127.68, 125.38, 118.43, 116.67, 112.18, 108.66, 85.97, 14.19; MS (ESI) m/z(%): 343 ([M+H]$^{+}$, 100%); purity (LC): >99%.

2-amino-4-(4-methylsulfanylphenyl)-6-phenylpyridine-3-carbonitrile, ***S4***

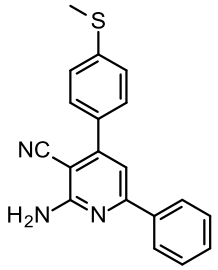

Yield: 0.701 g (34%); m.p. 197 °C; ^{1}H NMR (400 MHz, DMSO) δ 8.15 – 8.09 (m, 2H), 7.67 – 7.62 (m, 2H), 7.52 – 7.46 (m, 3H), 7.45 – 7.40 (m, 2H), 7.27 (s, 1H), 7.00 (s, 2H), 2.55 (s, 3H); ^{13}C NMR (101 MHz, DMSO) δ 160.91, 158.60, 154.24, 140.64, 137.58, 133.07, 130.06, 128.81, 128.61, 127.22, 125.57, 117.12, 109.00, 86.32, 14.30; MS (ESI) m/z(%): 318 ([M+H]$^{+}$, 100%); purity (LC): >99%.

2-amino-6-(4-methylsulfanylphenyl)-4-phenylpyridine-3-carbonitrile, ***S5***

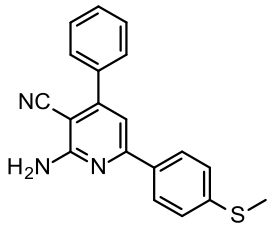

Yield: 0.688 g (33%); m.p. 153 °C; ^{1}H NMR (400 MHz, DMSO) δ 8.13 – 8.07 (m, 2H), 7.70 – 7.64 (m, 2H), 7.59 – 7.51 (m, 3H), 7.38 – 7.32 (m, 2H), 7.26 (s, 1H), 6.99 (s, 2H), 2.53 (s, 3H).; ^{13}C NMR (101 MHz, DMSO) δ 160.80, 157.99, 154.82, 141.19, 137.03, 133.76, 129.54, 128.70, 128.32, 127.63, 125.40, 117.09, 108.76, 86.31, 14.22; MS (ESI) m/z(%): 318 ([M+H]$^{+}$, 100%); purity (LC): >99%.

2-amino-4,6-bis(4-methylsulfanylphenyl)pyridine-3-carbonitrile, ***S6***

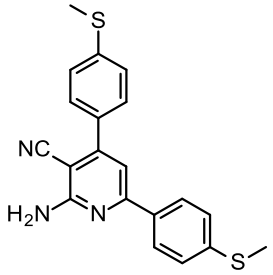

Yield: 0.538 g (23%); m.p. 142 °C; ^{1}H NMR (400 MHz, DMSO) δ 8.12 – 8.05 (m, 2H), 7.66 – 7.59 (m, 2H), 7.45 – 7.39 (m, 2H), 7.37 – 7.33 (m, 2H), 7.25 (s, 1H), 6.97 (s, 2H), 2.55 (s, 3H), 2.53 (s, 3H); ^{13}C NMR (101 MHz, DMSO) δ 160.86, 157.98, 154.18, 141.17, 140.59, 133.79, 133.12, 128.80, 127.62, 125.57, 125.39, 117.19, 108.52, 86.00, 14.31, 14.23; MS (ESI) m/z(%): 364 ([M+H]$^{+}$, 100%); purity (LC): >99%.

2-amino-6-(4-methoxyphenyl)-4-(4-methylsulfanylphenyl)pyridine-3-carbonitrile, ***S7***

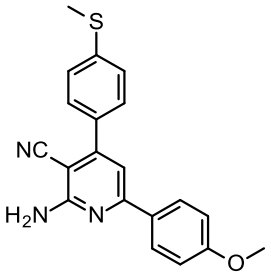

Yield: 0.833 g (80%); m.p. 195 °C; ^{1}H NMR (400 MHz, DMSO) δ 8.13 – 8.08 (m, 2H), 7.65 – 7.60 (m, 2H), 7.44 – 7.39 (m, 2H), 7.21 (s, 1H), 7.07 – 7.01 (m, 2H), 6.92 (s, 2H), 3.82 (s, 3H), 2.55 (s, 3H); ^{13}C NMR (101 MHz, DMSO) δ 160.97, 160.86, 158.27, 154.01, 140.49, 133.23, 129.91, 128.81, 128.78, 125.57, 117.31, 113.99, 108.21, 85.39, 55.31, 14.32; MS (ESI) m/z(%): 348 ([M+H]$^{+}$, 100%); purity (LC): >99%.

2-amino-4-(4-methoxyphenyl)-6-(4-methylsulfanylphenyl)pyridine-3-carbonitrile, ***S8***

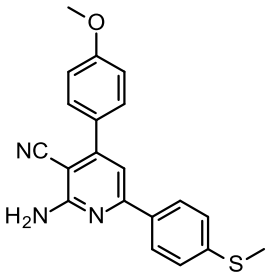

Yield: 1.021 g (55%); m.p. 150 °C; ^{1}H NMR (400 MHz, DMSO) δ 8.11 – 8.06 (m, 2H), 7.67 – 7.62 (m, 2H), 7.37 – 7.32 (m, 2H), 7.23 (s, 1H), 7.13 – 7.08 (m, 2H), 6.93 (s, 2H), 3.84 (s, 3H), 2.53 (s, 3H); ^{13}C NMR (101 MHz, DMSO) δ 160.90, 160.39, 157.82, 154.38, 141.06, 133.88, 129.83, 129.11, 127.61, 125.39, 117.38, 114.13, 108.56, 86.07, 55.35, 14.24; MS (ESI) m/z(%): 348 ([M+H]$^{+}$, 100%); purity (LC): >98%.

NMR spectra of synthesized 2-amino-4,6-diphenylpyridine-3-carbonitrile derivatives

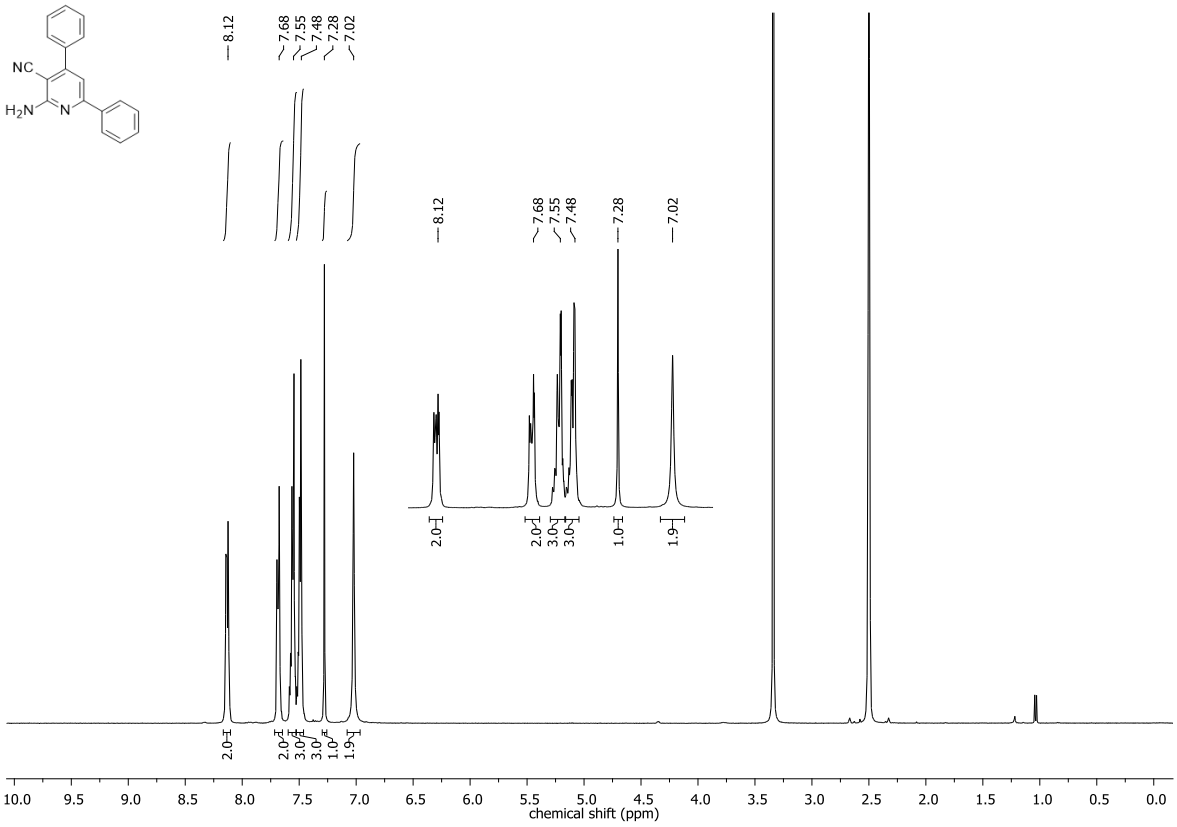

Figure S.1. ^{1}H NMR spectrum of 2-amino-4,6-diphenylpyridine-3-carbonitrile **S1**.

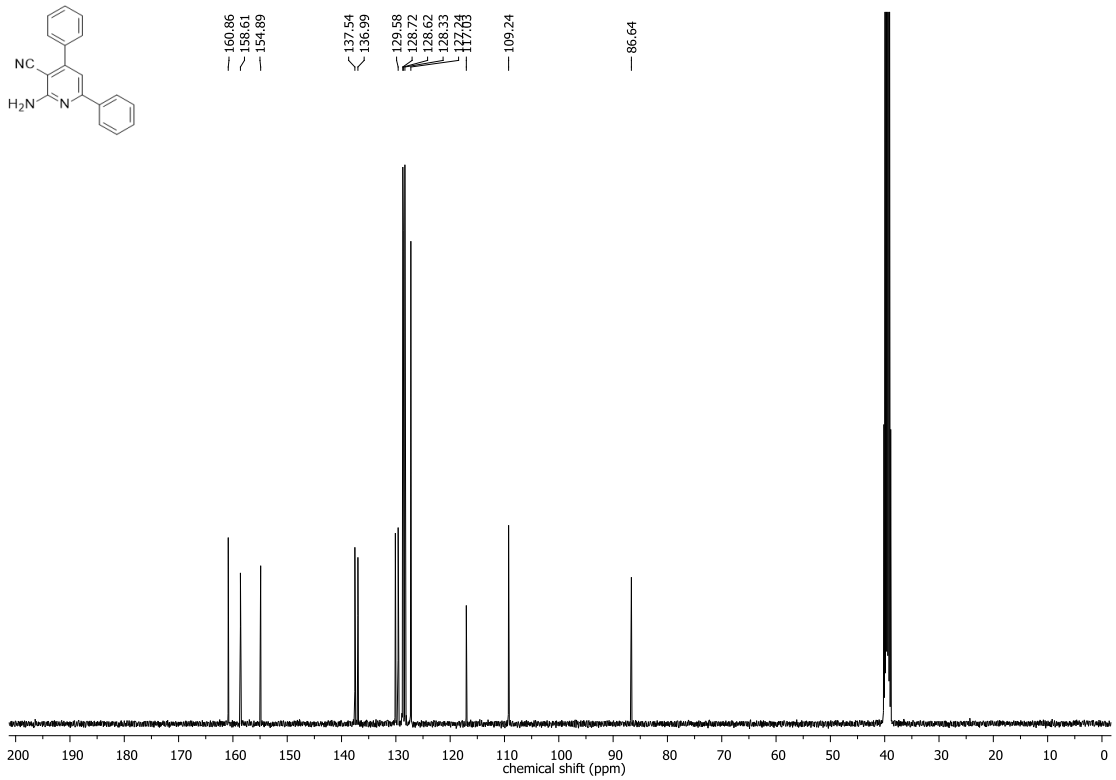

Figure S.2. ^{13}C NMR spectrum of 2-amino-4,6-diphenylpyridine-3-carbonitrile **S1**.

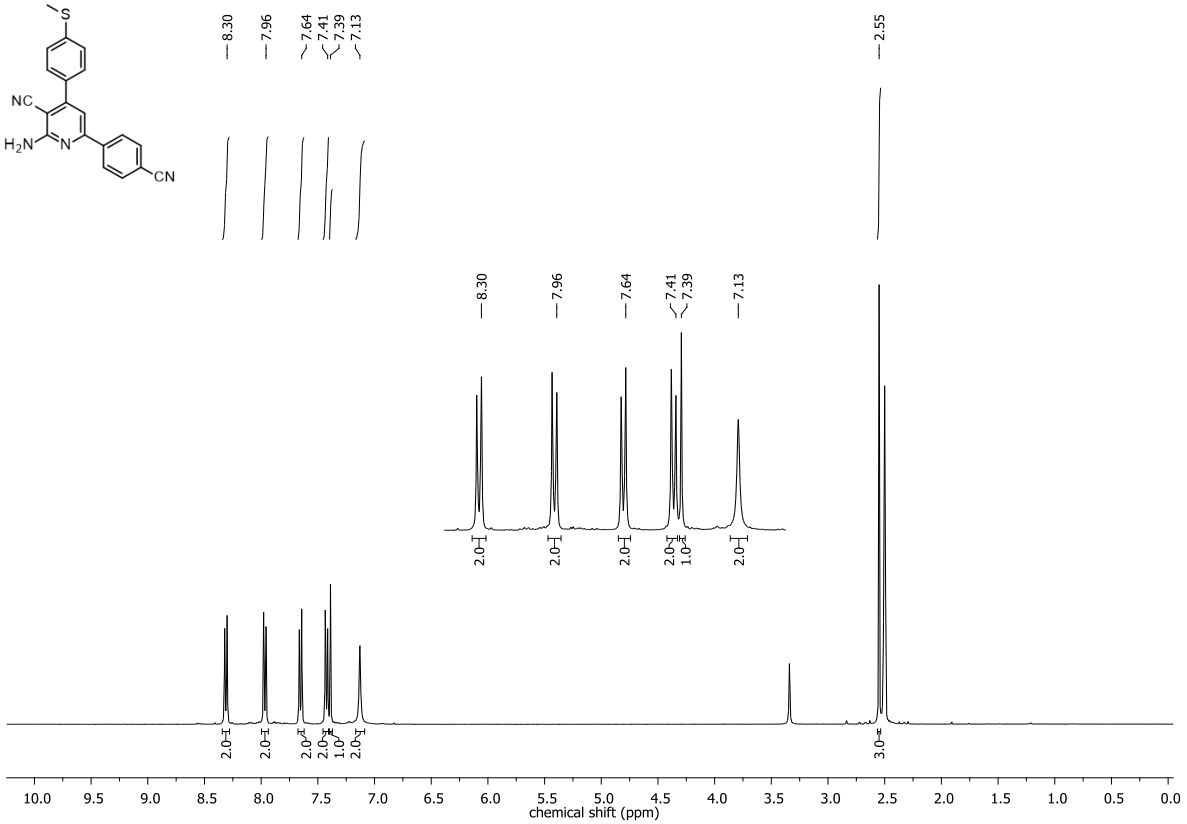

Figure S.3. ^{1}H NMR spectrum of 2-amino-6-(4-cyanophenyl)-4-(4-methylsulfanylphenyl)pyridine-3-carbonitrile **S2**.

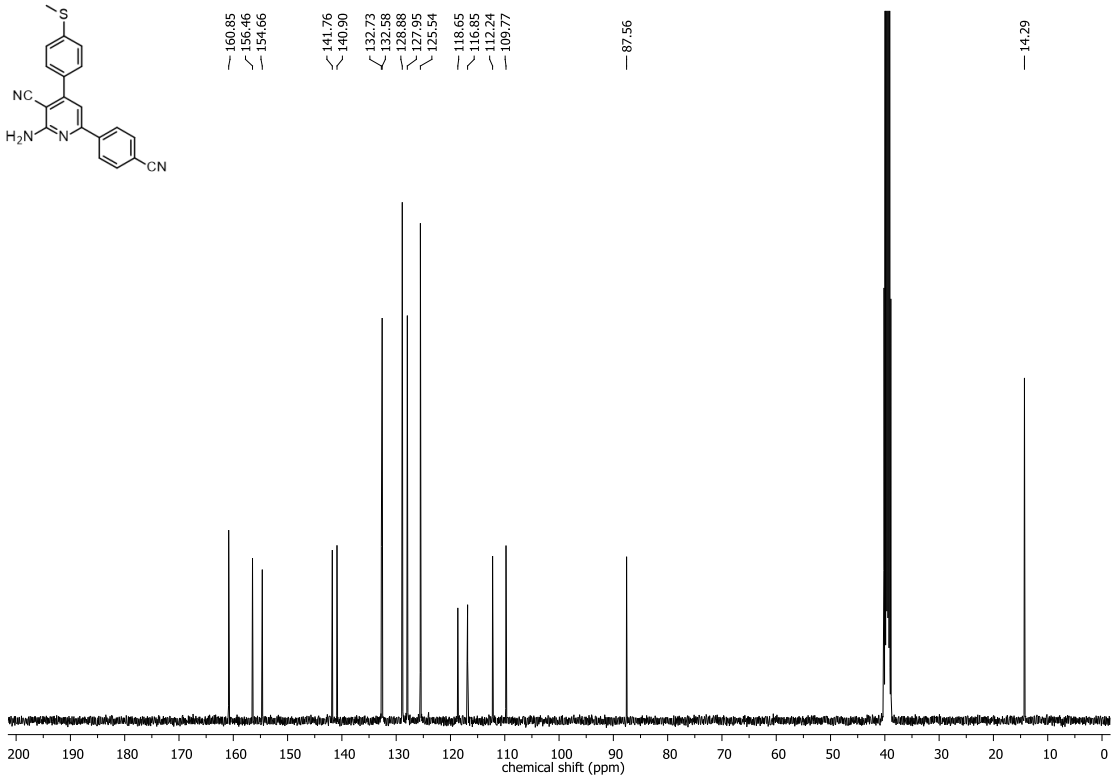

Figure S.4. ^{13}C NMR spectrum of 2-amino-6-(4-cyanophenyl)-4-(4-methylsulfanylphenyl)pyridine-3-carbonitrile **S2**.

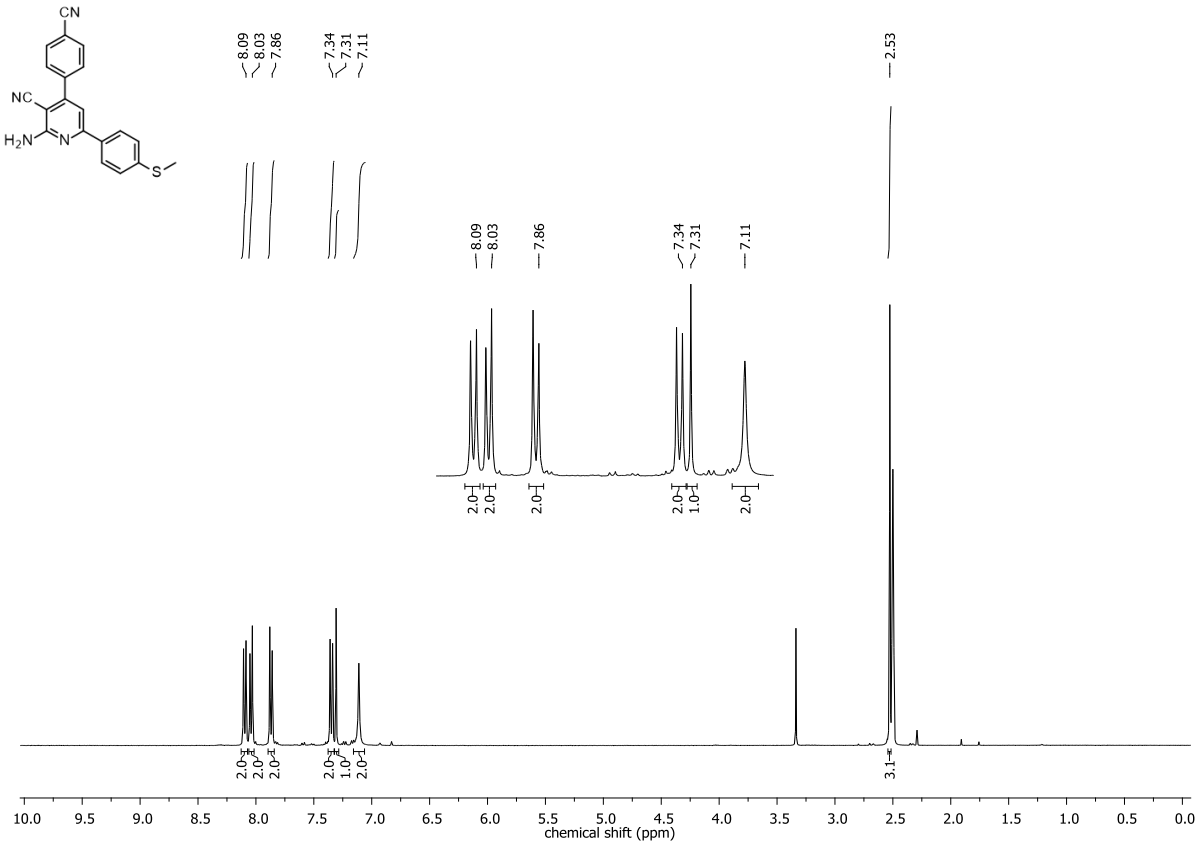

Figure S.5. ^{1}H NMR spectrum of 2-amino-4-(4-cyanophenyl)-6-(4-methylsulfanylphenyl)pyridine-3-carbonitrile **S3**.

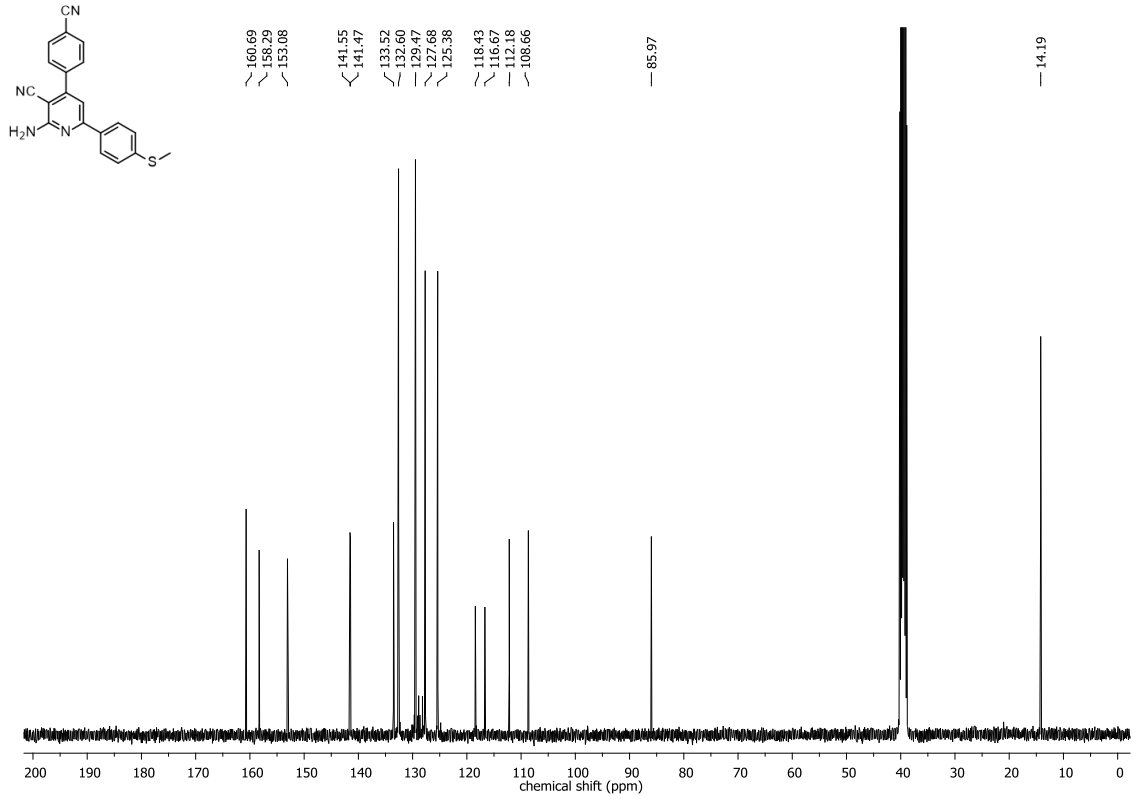

Figure S.6. ^{13}C NMR spectrum of 2-amino-4-(4-cyanophenyl)-6-(4-methylsulfanylphenyl)pyridine-3-carbonitrile **S3**.

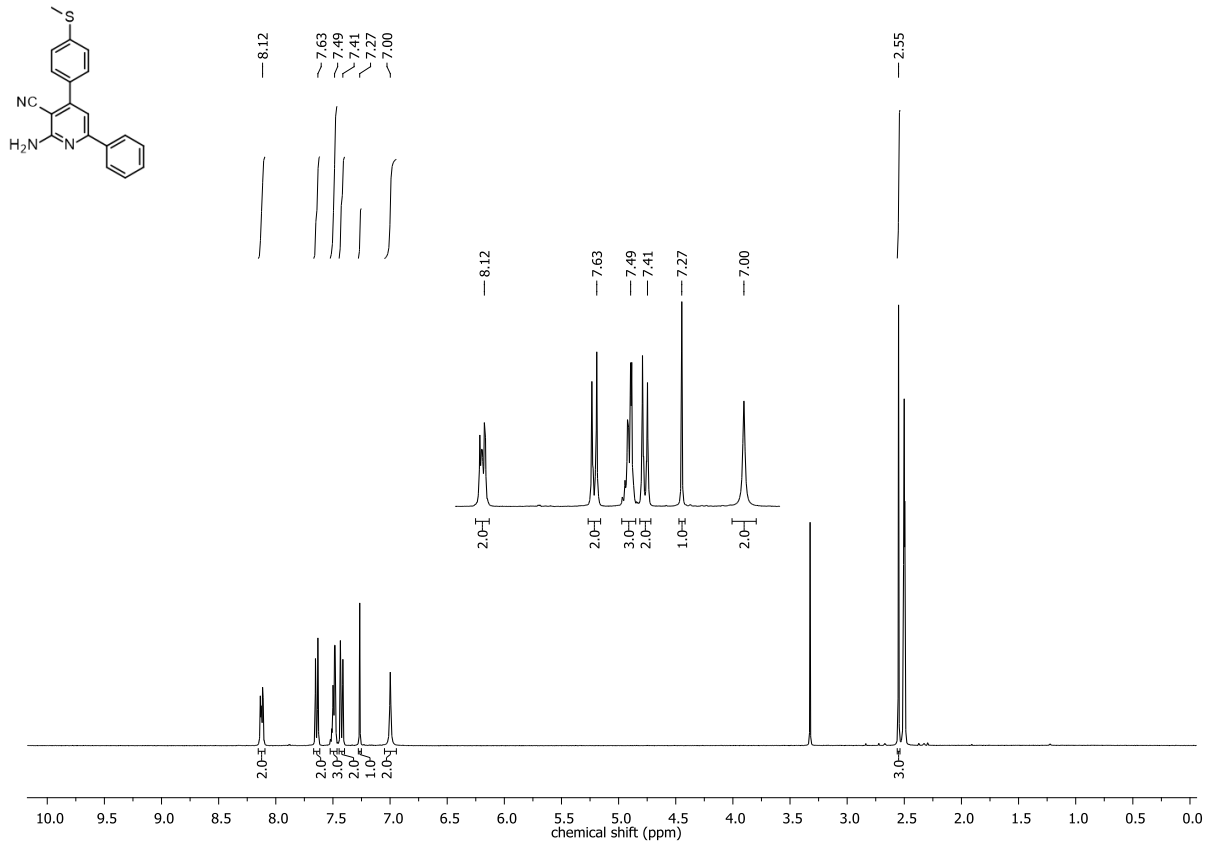

Figure S.7. ^{1}H NMR spectrum of 2-amino-4-(4-methylsulfanylphenyl)-6-phenylpyridine-3-carbonitrile **S4**.

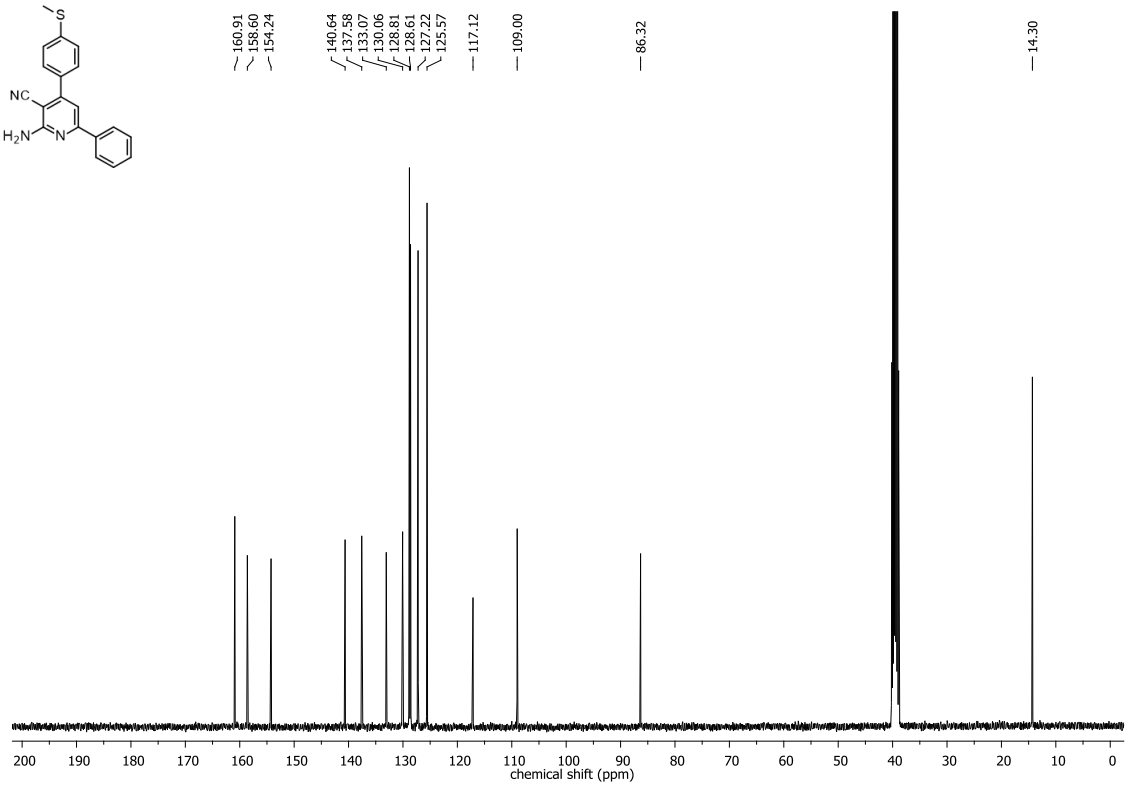

Figure S.8. ^{13}C NMR spectrum of 2-amino-4-(4-methylsulfanylphenyl)-6-phenylpyridine-3-carbonitrile **S4**.

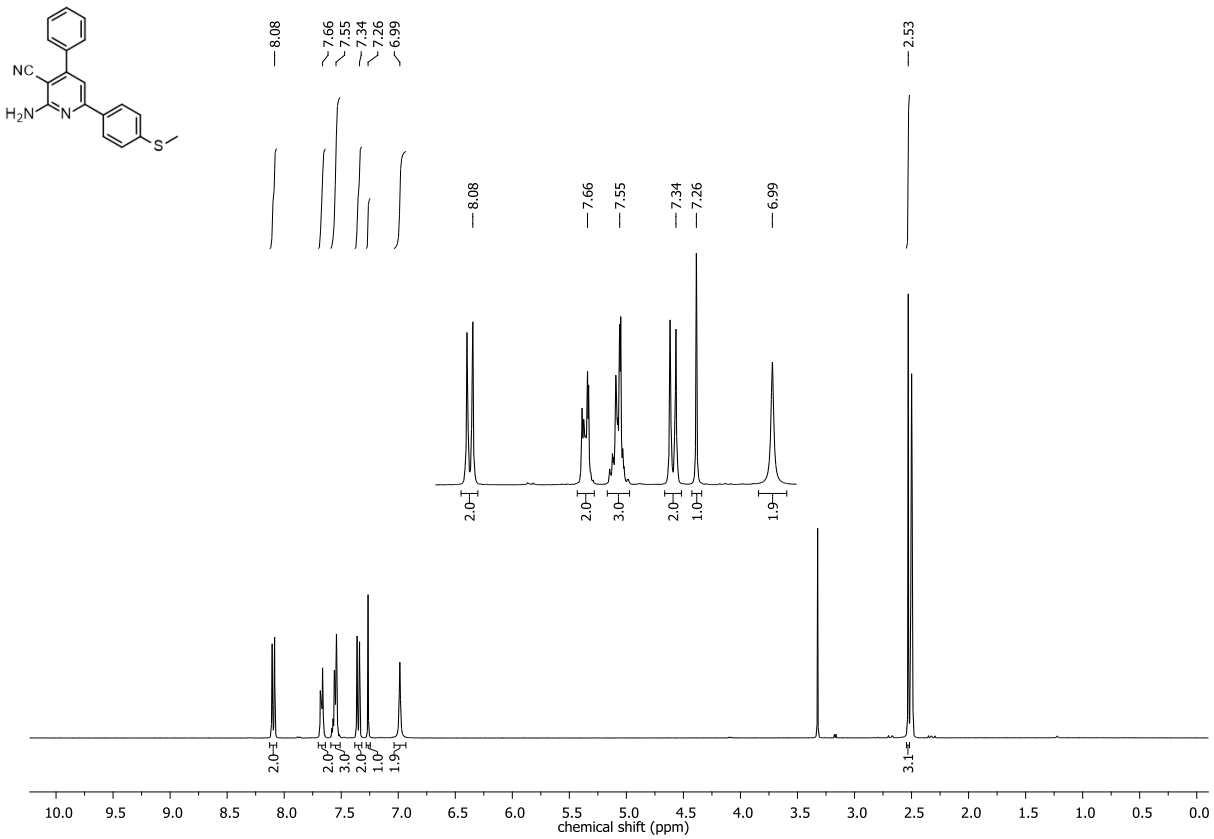

Figure S.9. ^{1}H NMR spectrum of 2-amino-6-(4-methylsulfanylphenyl)-4-phenylpyridine-3-carbonitrile **S5**.

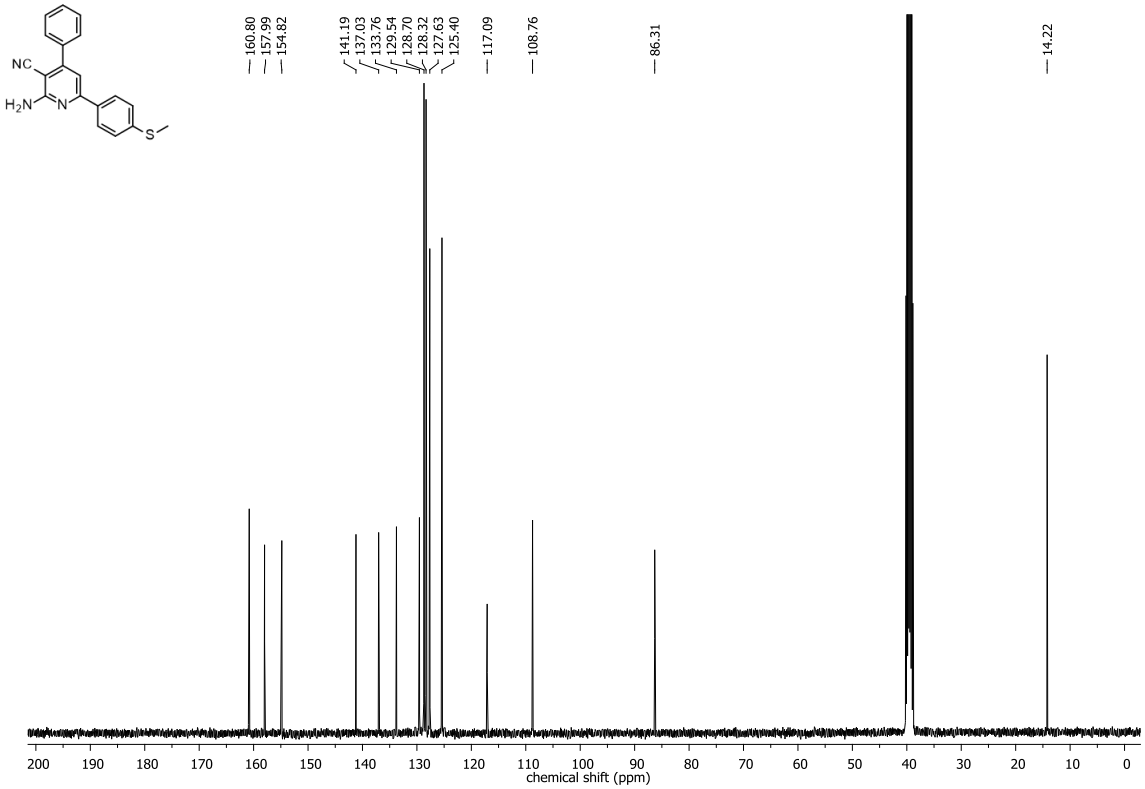

Figure S.10. ^{13}C NMR spectrum of 2-amino-6-(4-methylsulfanylphenyl)-4-phenylpyridine-3-carbonitrile **S5**.

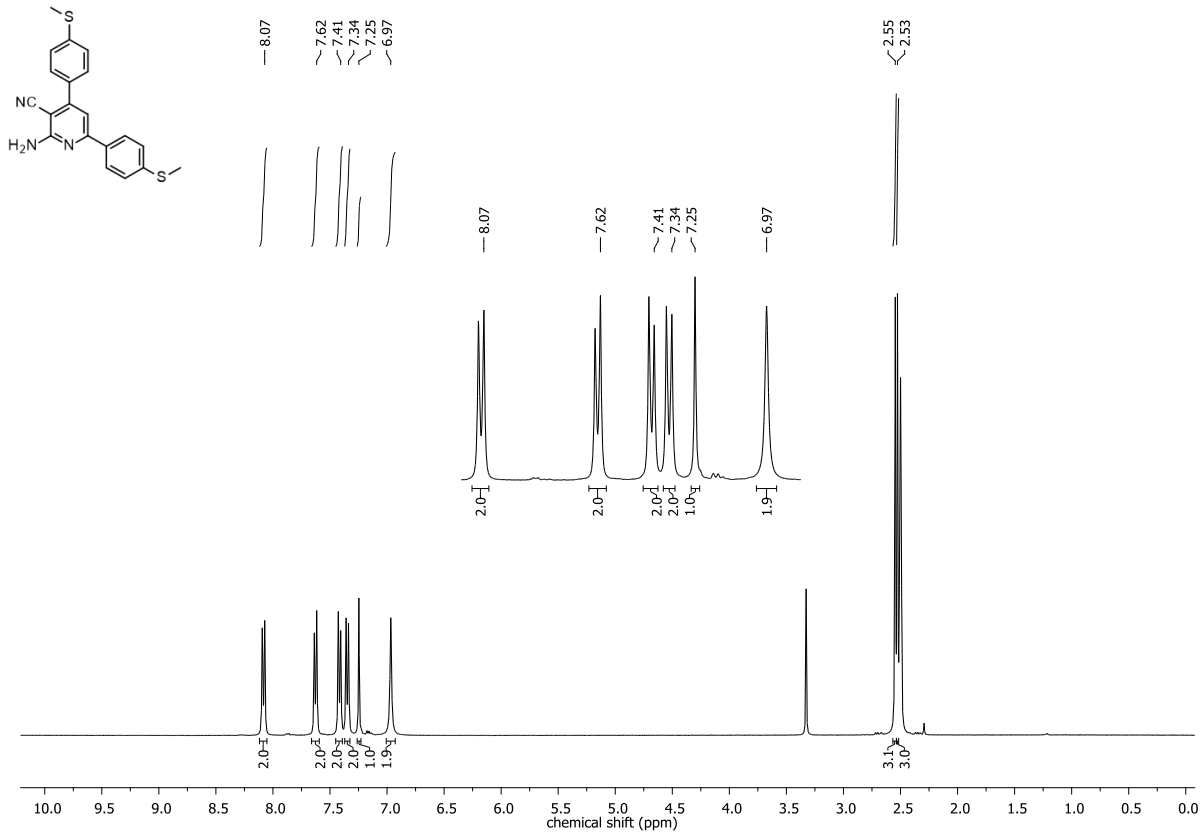

Figure S.11. ^{1}H NMR spectrum of 2-amino-4,6-bis(4-methylsulfanylphenyl)pyridine-3-carbonitrile **S6**.

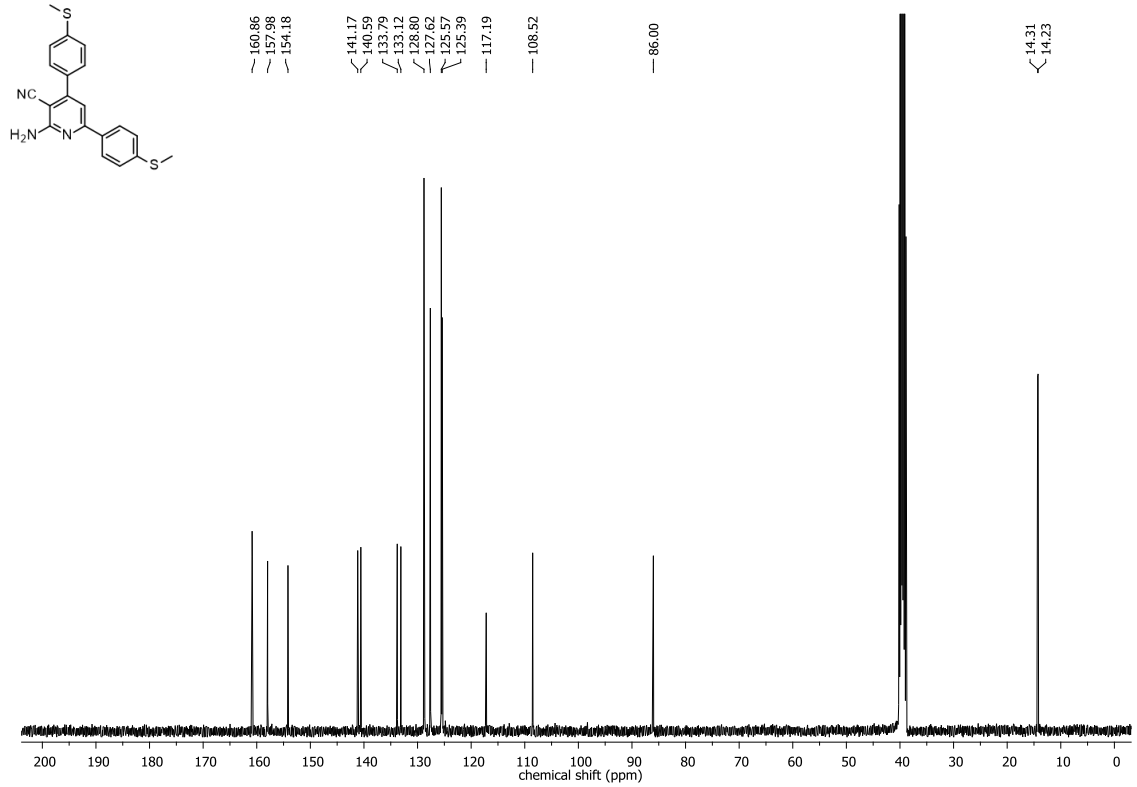

Figure S.12. ^{13}C NMR spectrum of 2-amino-4,6-bis(4-methylsulfanylphenyl)pyridine-3-carbonitrile **S6**.

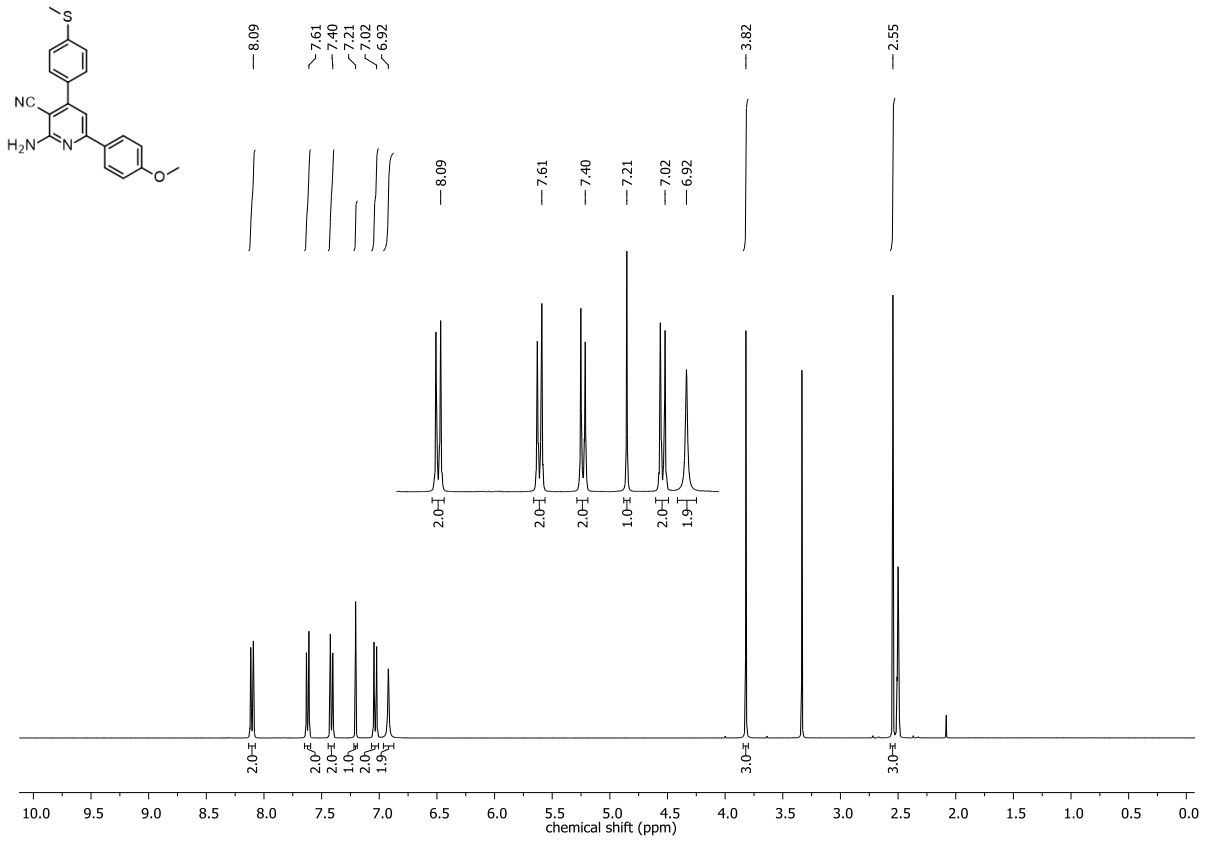

Figure S.13. ^{1}H NMR spectrum of 2-amino-6-(4-methoxyphenyl)-4-(4-methylsulfanylphenyl)pyridine-3-carbonitrile **S7**.

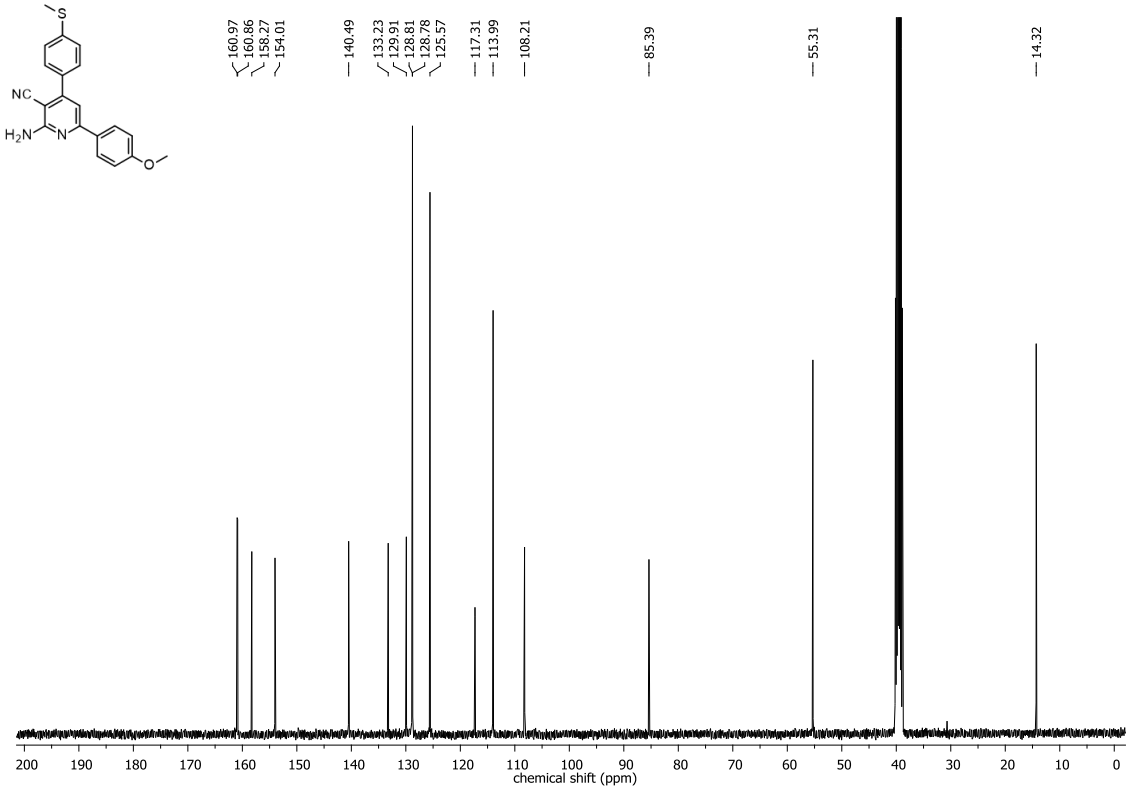

Figure S.14. ^{13}C NMR spectrum of 2-amino-6-(4-methoxyphenyl)-4-(4-methylsulfanylphenyl)pyridine-3-carbonitrile **S7**.

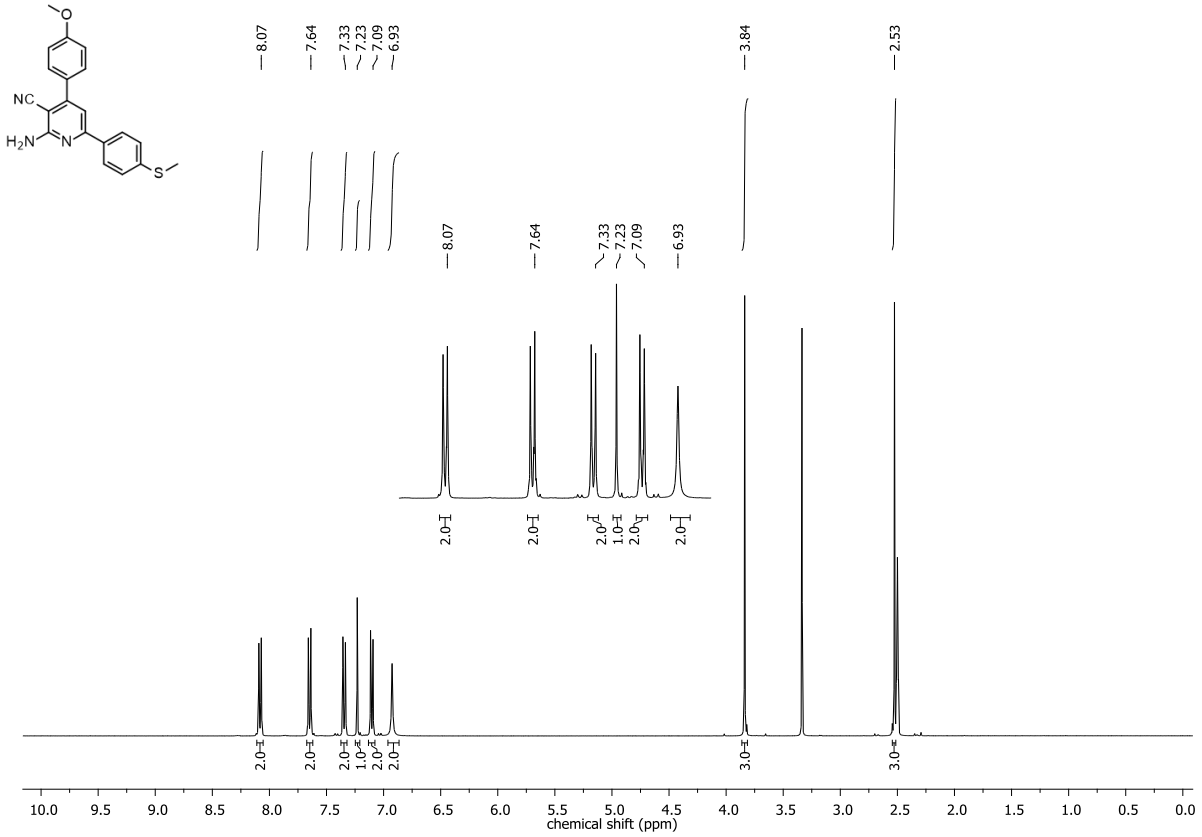

Figure S.15. ^{1}H NMR spectrum of 2-amino-4-(4-methoxyphenyl)-6-(4-methylsulfanylphenyl)pyridine-3-carbonitrile **S8**.

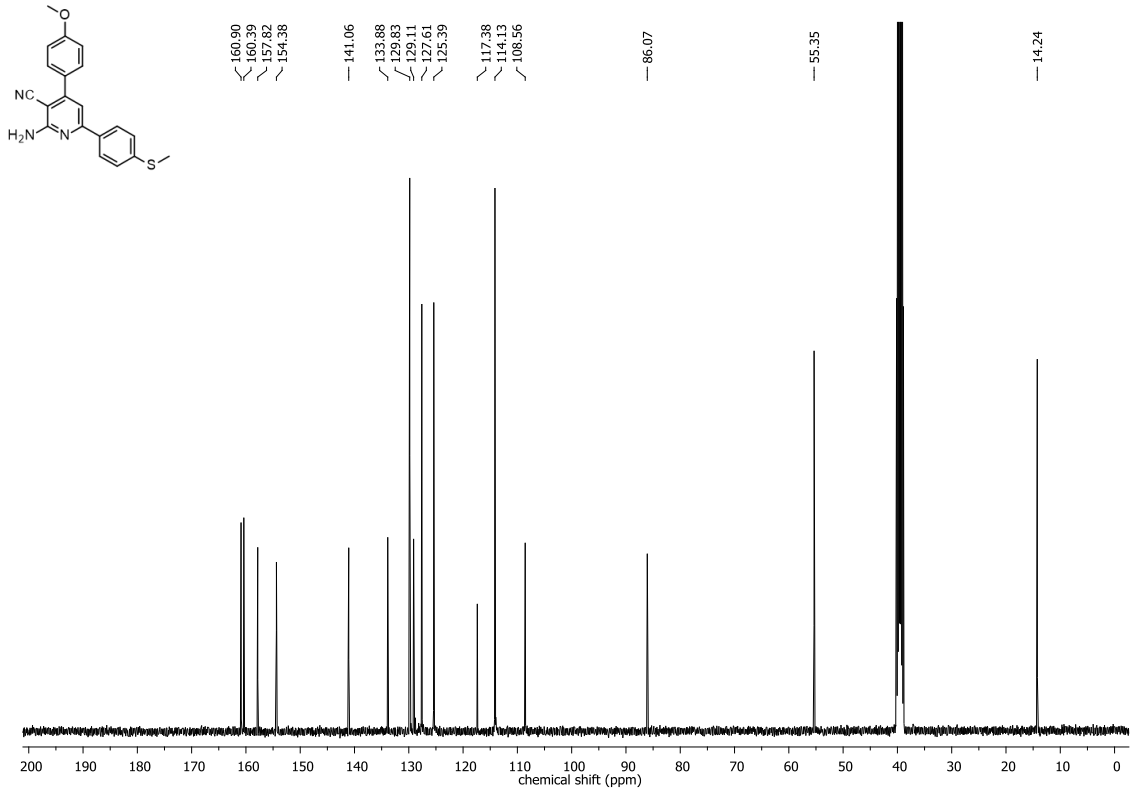

Figure S.16. ^{13}C NMR spectrum of 2-amino-4-(4-methoxyphenyl)-6-(4-methylsulfanylphenyl)pyridine-3-carbonitrile **S8**.

Cyclic voltammetry curves showing oxidation and reduction processes of 2-amino-4,6-diphenylpyridine-3-carbonitrile derivatives in acetonitrile

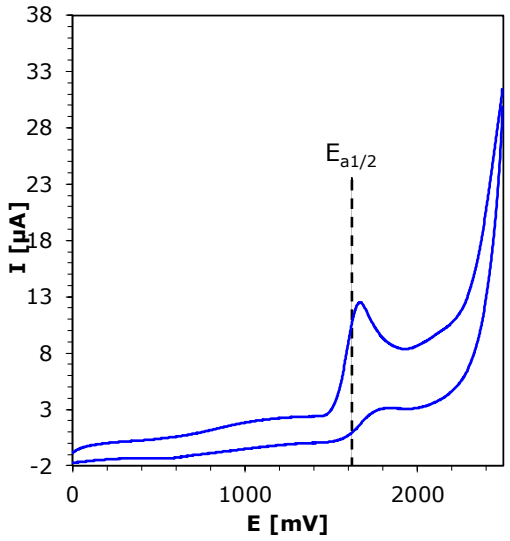

Figure S.17. Cyclic voltammogram curves of the S1 oxidation in acetonitrile.

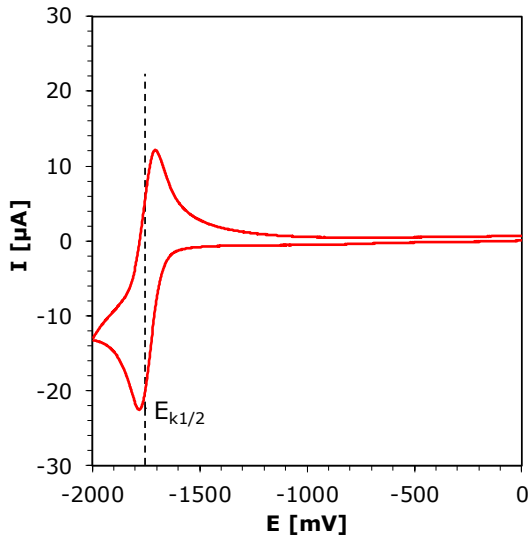

Figure S.18. Cyclic voltammogram curves of the S1 reduction in acetonitrile.

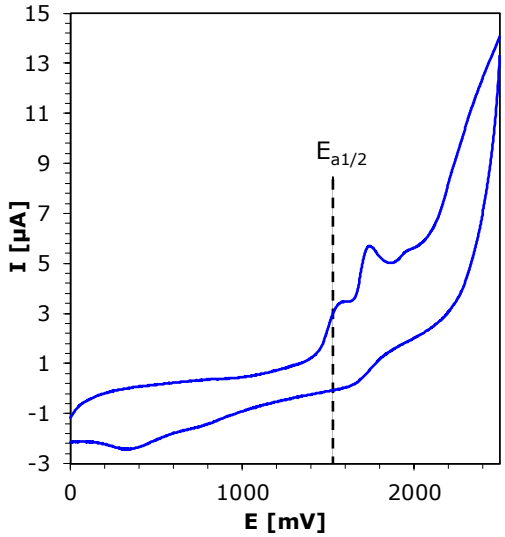

Figure S.19. Cyclic voltammogram curves of the S2 oxidation in acetonitrile.

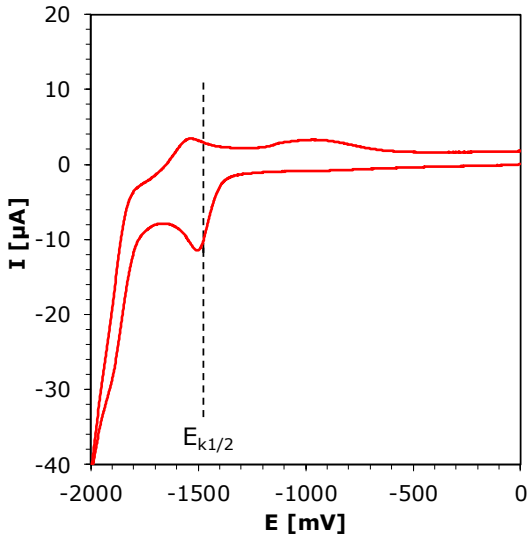

Figure S.20. Cyclic voltammogram curves of the S2 reduction in acetonitrile.

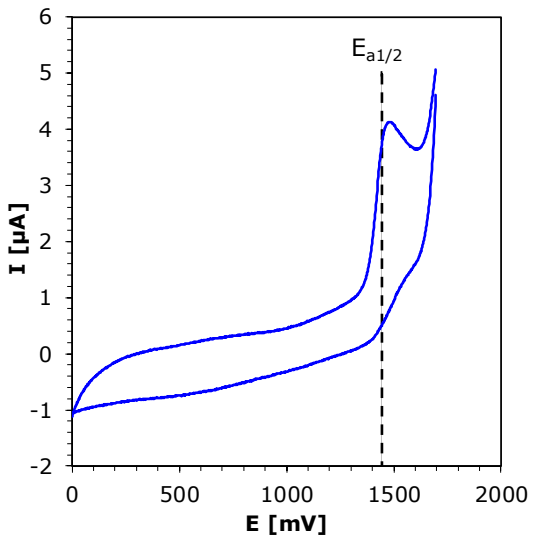

Figure S.21. Cyclic voltammogram curves of the S3 oxidation in acetonitrile.

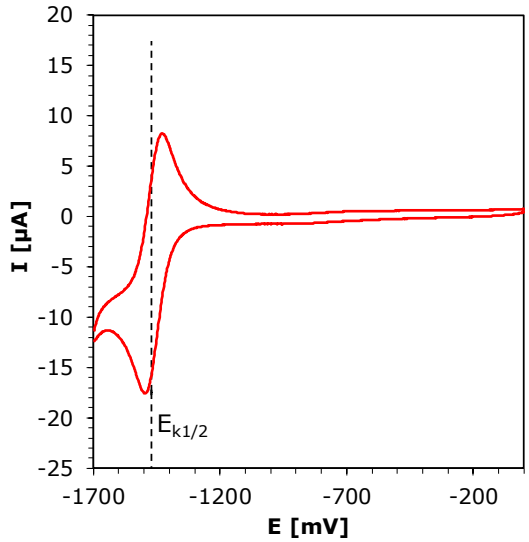

Figure S.22. Cyclic voltammogram curves of the S3 reduction in acetonitrile.

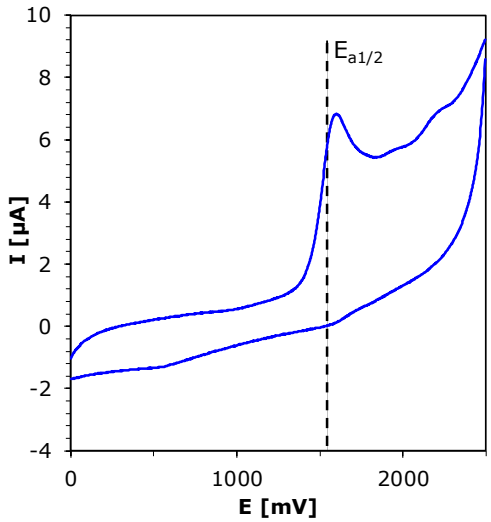

Figure S.23. Cyclic voltammogram curves of the S4 oxidation in acetonitrile.

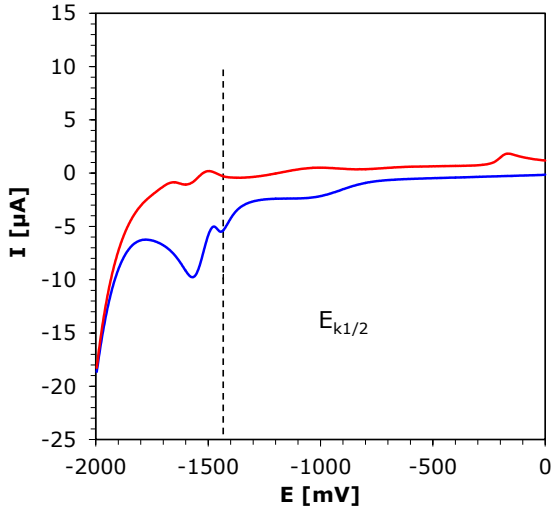

Figure S.24. Cyclic voltammogram curves of the S4 reduction in acetonitrile.

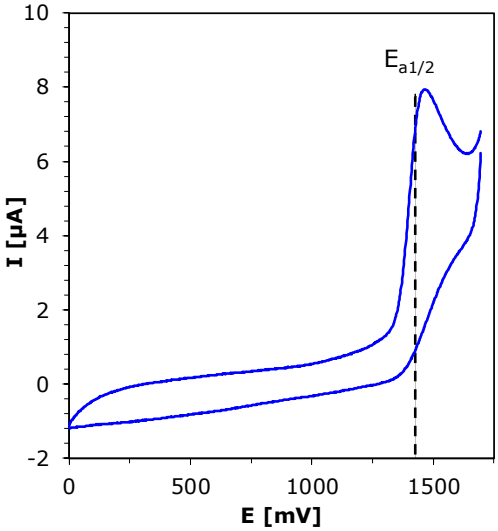

Figure S.25. Cyclic voltammogram curves of

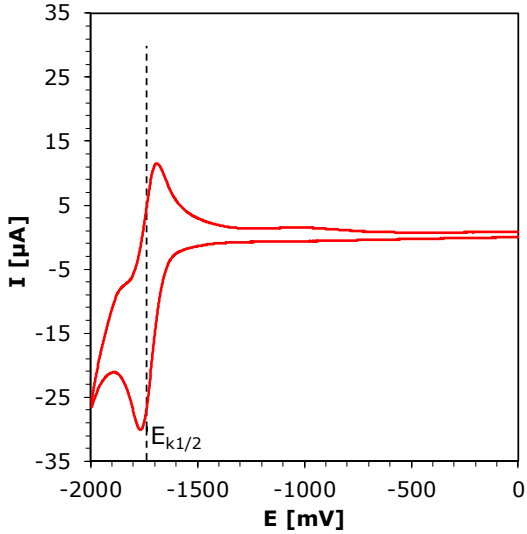

Figure S.26. Cyclic voltammogram curves of the

the S5 oxidation in acetonitrile.

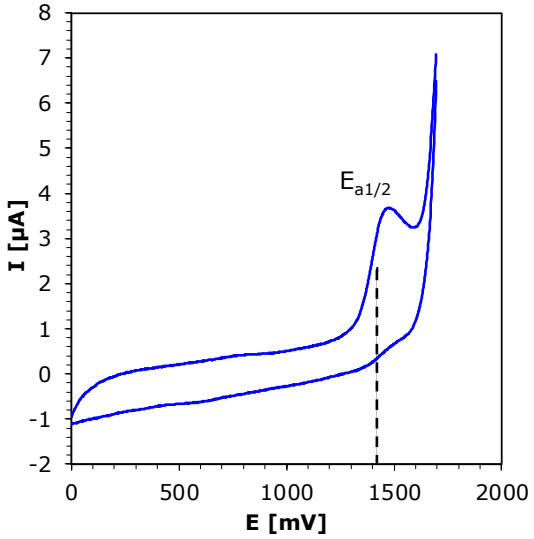

Figure S.27. Cyclic voltammogram curves of the S6 oxidation in acetonitrile.

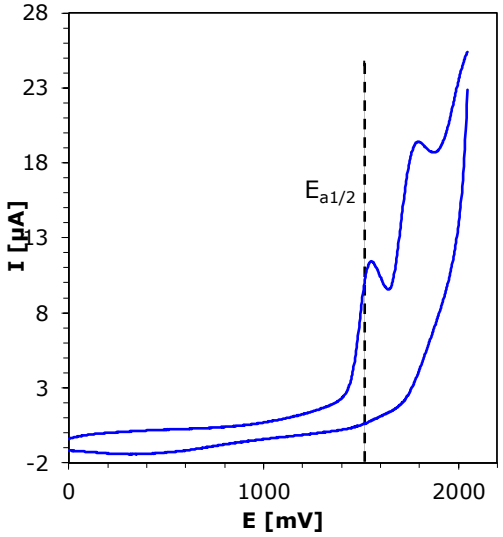

Figure S.29. Cyclic voltammogram curves of the S7 oxidation in acetonitrile.

S5 reduction in acetonitrile.

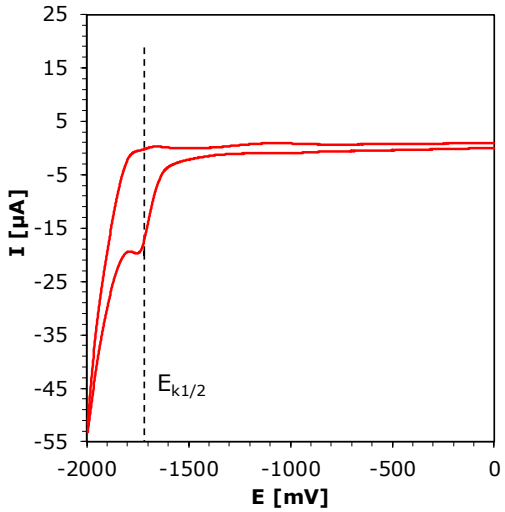

Figure S.28. Cyclic voltammogram curves of the S6 reduction in acetonitrile.

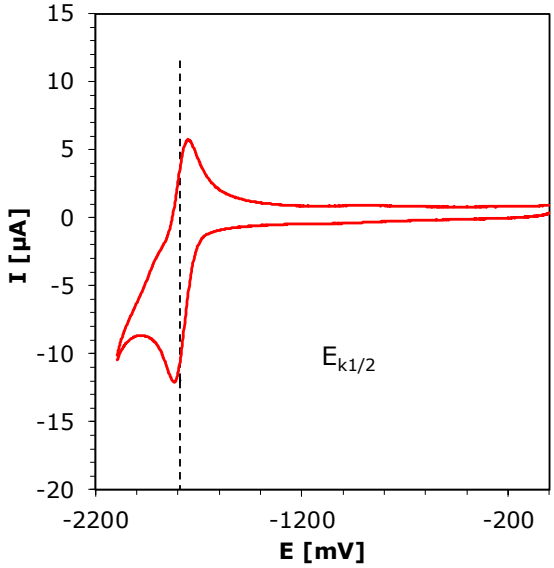

Figure S.30. Cyclic voltammogram curves of the S7 reduction in acetonitrile.

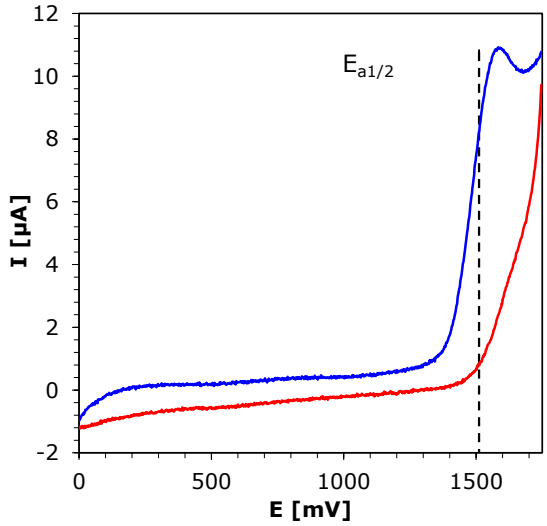

Figure S.31. Cyclic voltammogram curves of the S8 oxidation in acetonitrile.

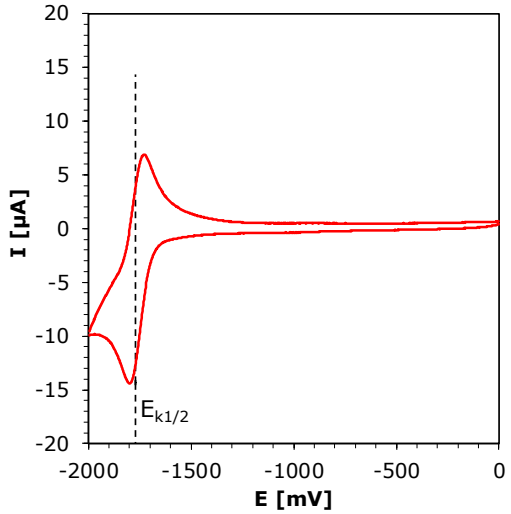

Figure S.32. Cyclic voltammogram curves of the S8 reduction in acetonitrile.

Absorption and fluorescence spectra for the determination of the excited singlet state energy for investigated of 2-amino-4,6-diphenylpyridine-3-carbonitrile derivatives in acetonitrile.

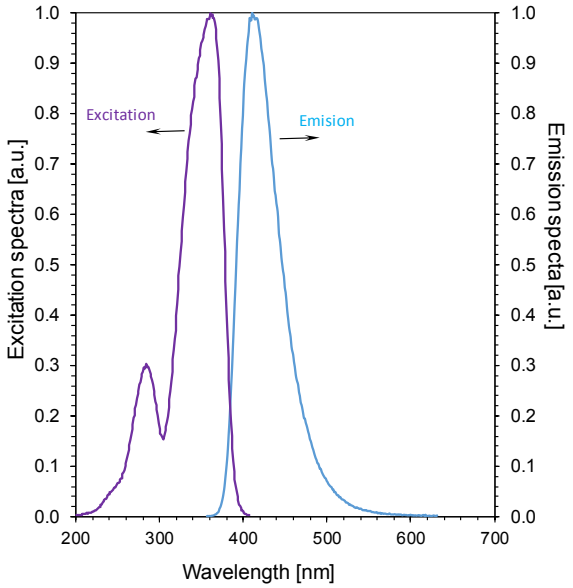

Figure S.33. Absorption and fluorescence spectra for the determination of the excited singlet state energy for S1 derivative.

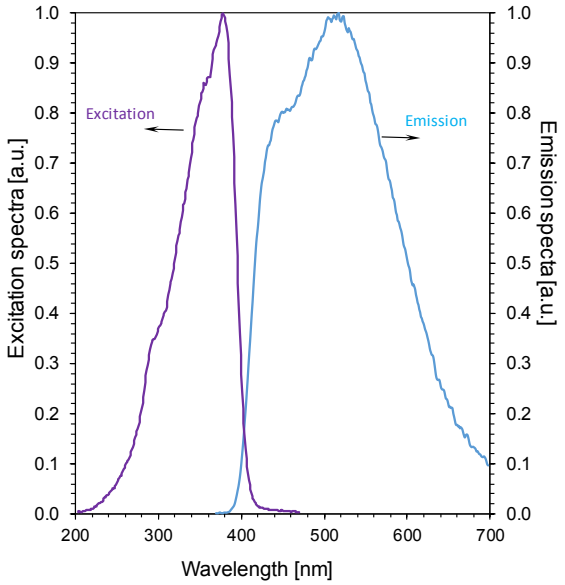

Figure S.34. Absorption and fluorescence spectra for the determination of the excited singlet state energy for S2 derivative.

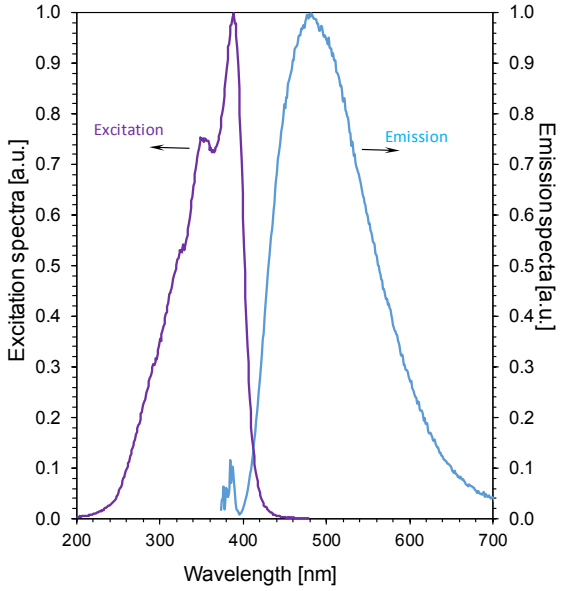

Figure S.35. Absorption and fluorescence spectra for the determination of the excited singlet state energy for S3 derivative.

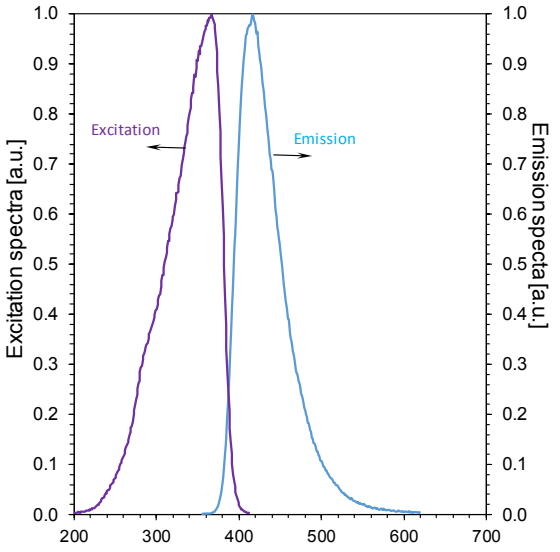

Figure S.36. Absorption and fluorescence spectra for the determination of the excited singlet state energy for S4 derivative.

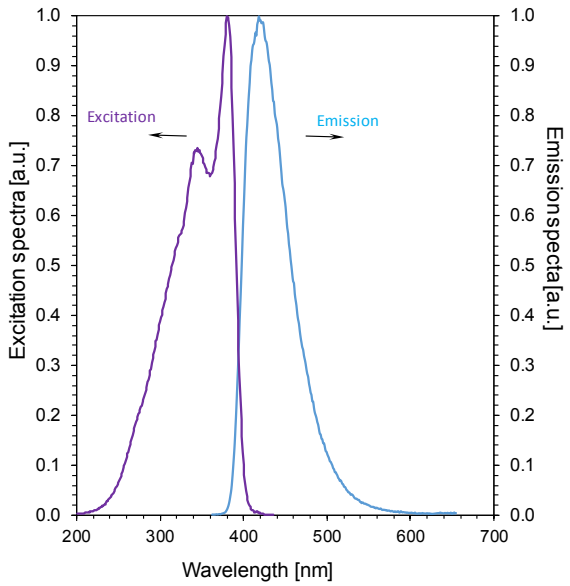

Figure S.37. Absorption and fluorescence spectra for the determination of the excited singlet state energy for S5 derivative.

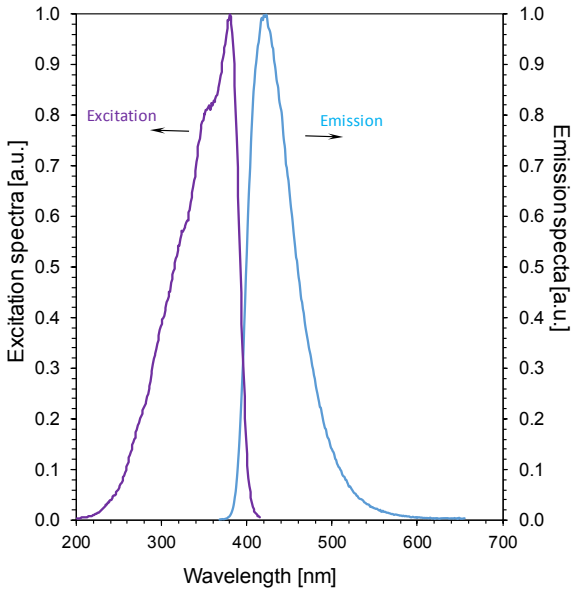

Figure S.38. Absorption and fluorescence spectra for the determination of the excited singlet state energy for S6 derivative.

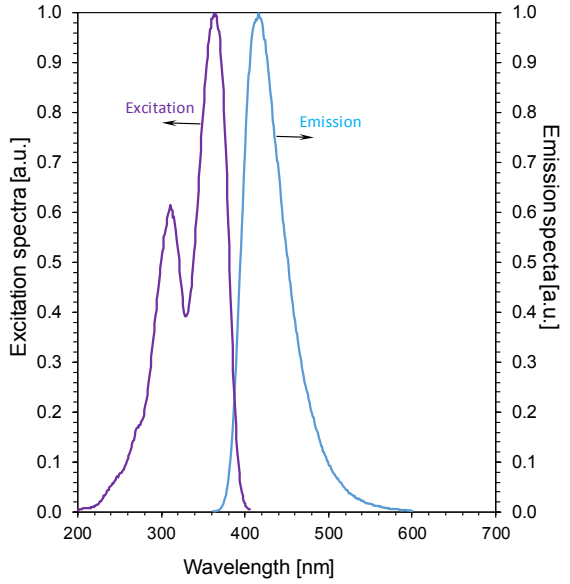

Figure S.39. Absorption and fluorescence spectra for the determination of the excited singlet state energy for S7 derivative.

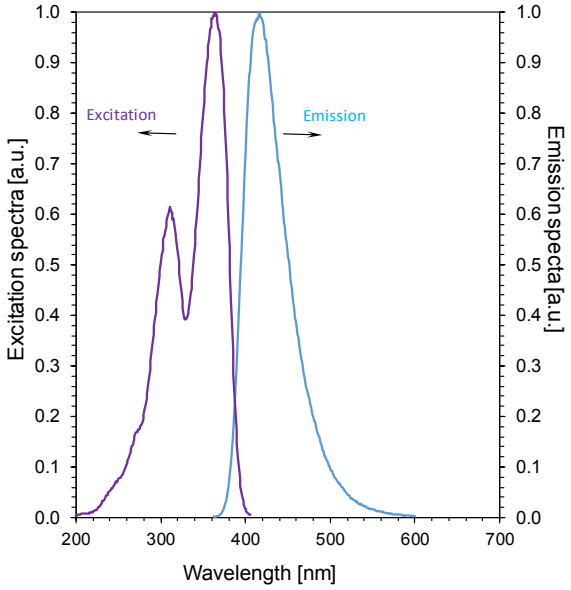

Figure S.40. Absorption and fluorescence spectra for the determination of the excited singlet state energy for S8 derivative.

The optimized structures and HOMO and LUMO orbitals of investigated 2-amino-4,6-diphenylpyridine-3-carbonitrile derivatives free molecules determined with the use of uB3LYP/6-31G* level of theory

Compound	HOMO	LUMO
2-amino-4,6-diphenylpyridine-3-carbonitrile 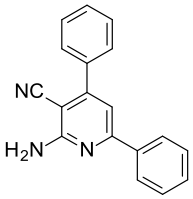 S1(PHT20-002)	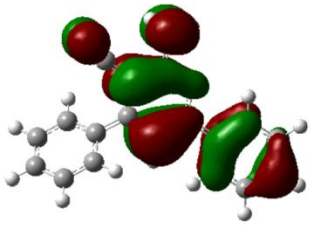	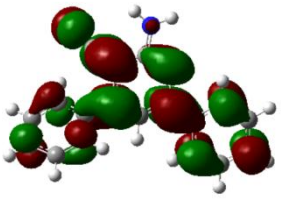
2-amino-6-(4-cyanophenyl)-4-(4-methylsulfanylphenyl)-pyridine-3-carbonitrile 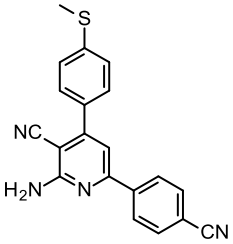 S2(P104)	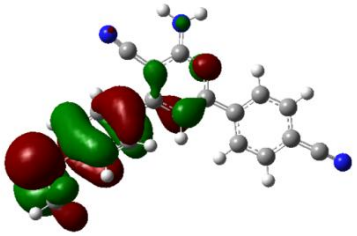	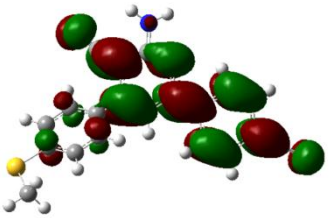
2-amino-4-(4-cyanophenyl)-6-(4-methylsulfanylphenyl)-pyridine-3-carbonitrile 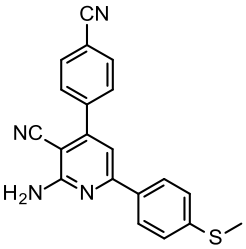 S3(P106)	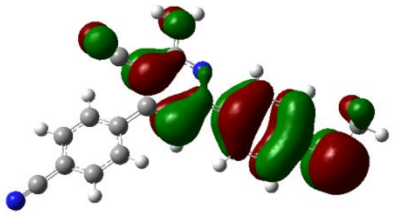	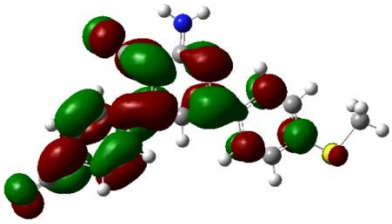
2-amino-4-(4-methylsulfanylphenyl)-6-phenylpyridine-3-carbonitrile 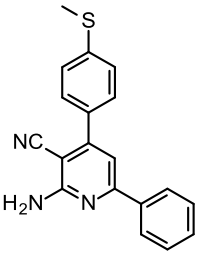 S4 (P109)	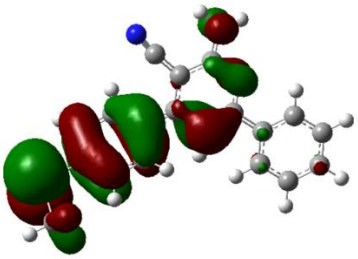	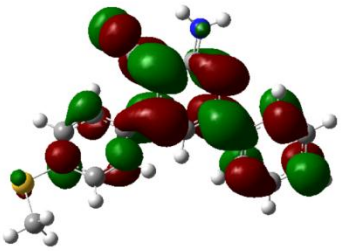

2-amino-6-(4-methylsulfanylphenyl)-4-phenylpyridine-3-carbonitrile, 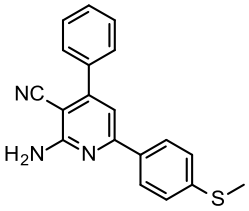 S5(P110)	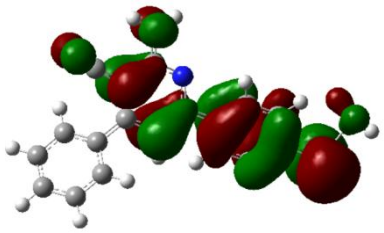	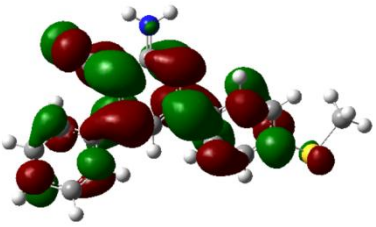
2-amino-4,6-bis(4-methylsulfanylphenyl)pyridine-3-carbonitrile 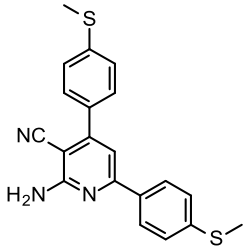 S6(P111)	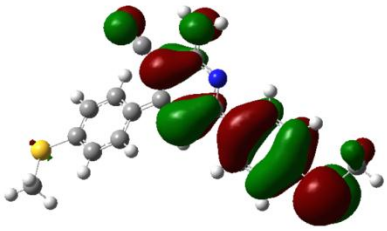	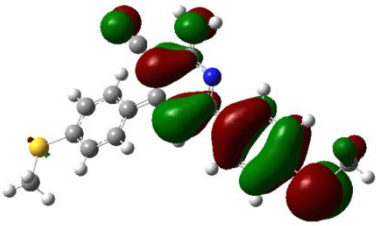
2-amino-6-(4-methoxyphenyl)-4-(4-methylsulfanylphenyl)-pyridine-3-carbonitrile 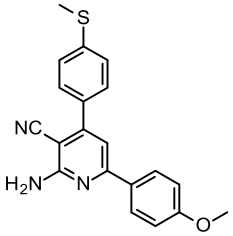 S7(PK06-022)	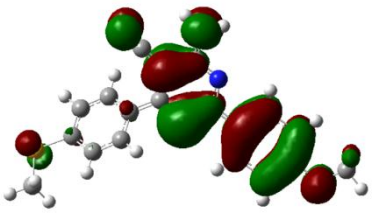	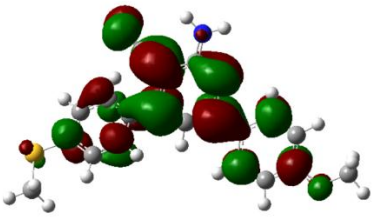
2-amino-4-(4-methoxyphenyl)-6-(4-methylsulfanylphenyl)-pyridine-3-carbonitrile 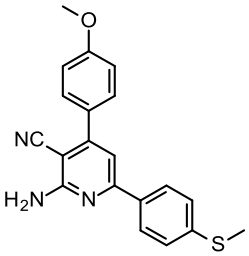 S8(PK06-048)	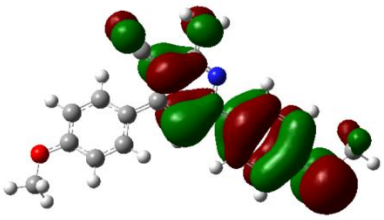	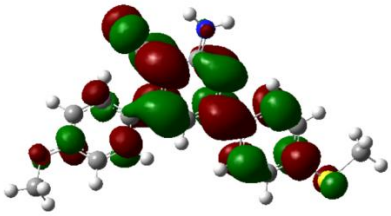

Fluorescence quenching with Speedcure 938 of investigated 2-amino-4,6-diphenylpyridine-3-carbonitrile derivatives together with Stern-Volmer correlation

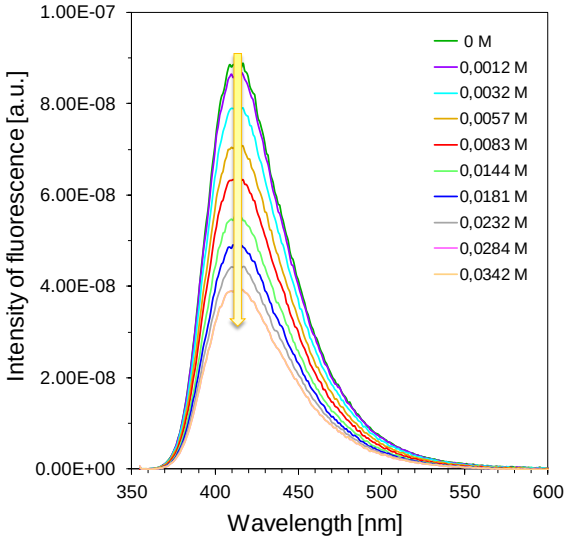

Figure S.41. Fluorescence quenching of S1

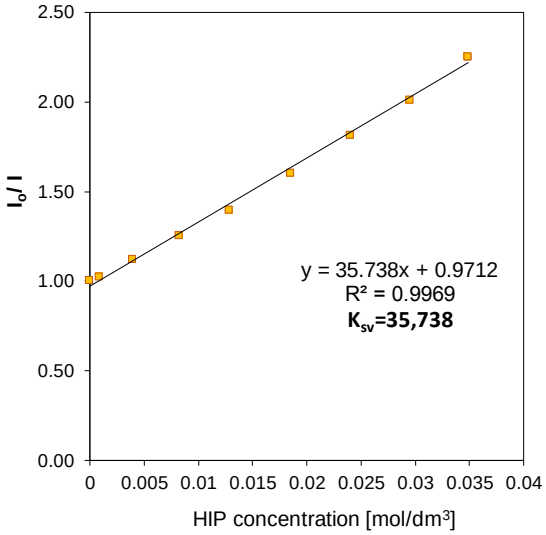

Figure S.42. Stern-Volmer treatment for the S1/HIP fluorescence quenching.

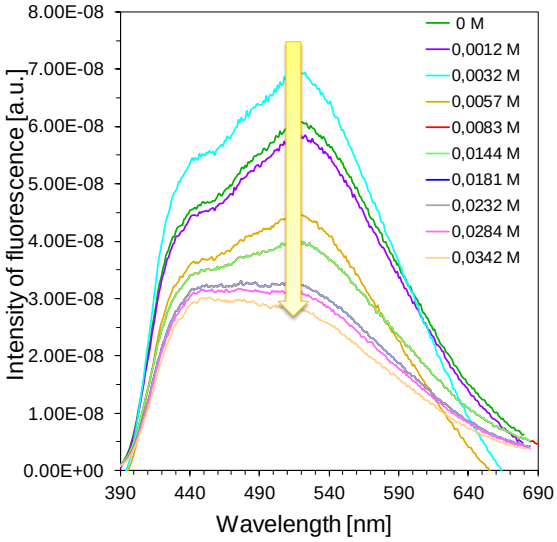

Figure S.43. Fluorescence quenching of S2.

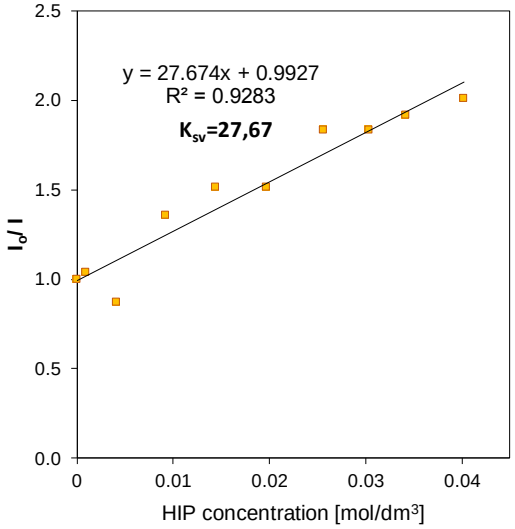

Figure S.44. Stern-Volmer treatment for the S2/HIP fluorescence quenching.

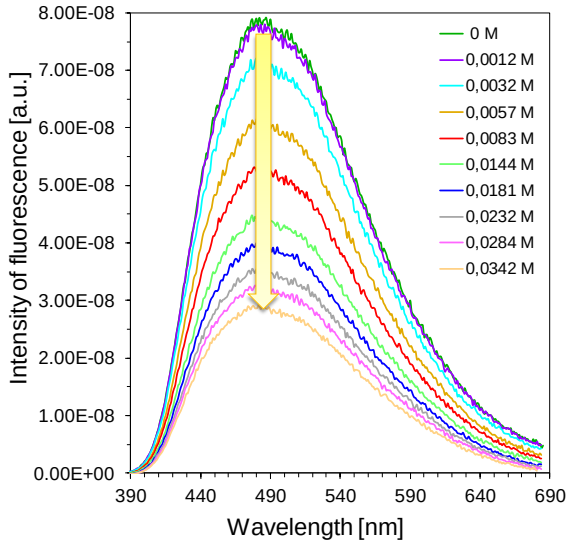

Figure S.45. Fluorescence quenching of S3.

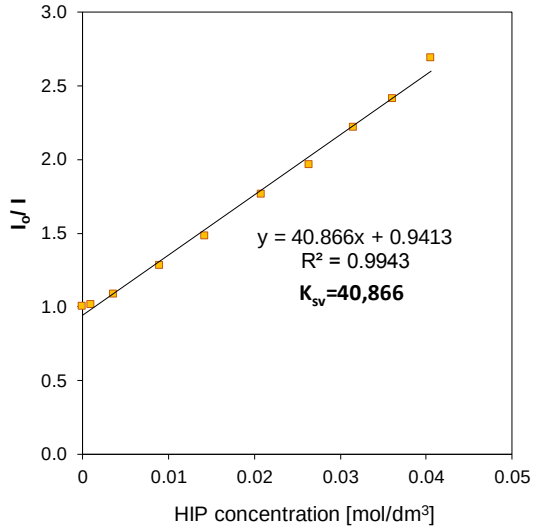

Figure S.46. Stern-Volmer treatment for the S3/HIP fluorescence quenching.

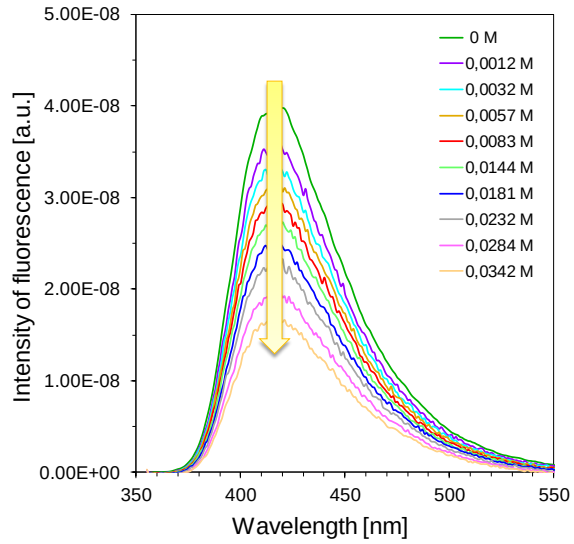

Figure S.47. Fluorescence quenching of S4.

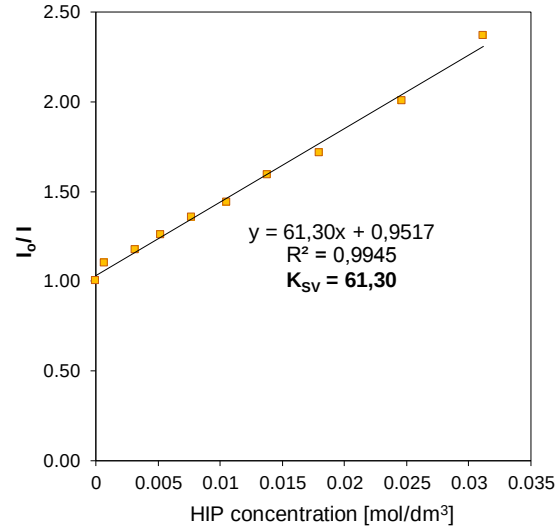

Figure S.48. Stern-Volmer treatment for the S4/HIP fluorescence quenching.

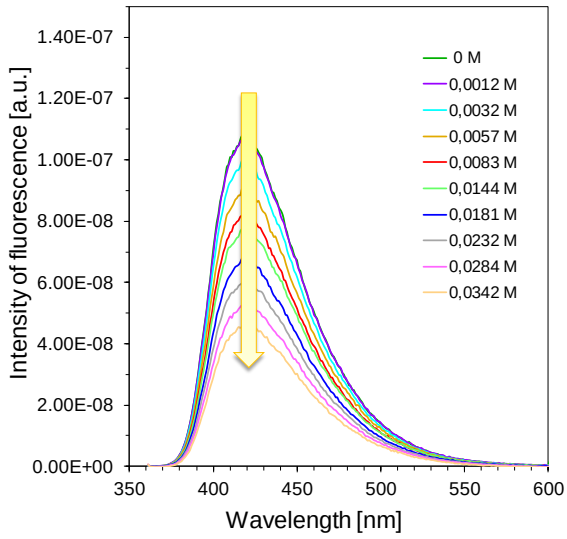

Figure S.49. Fluorescence quenching of S5.

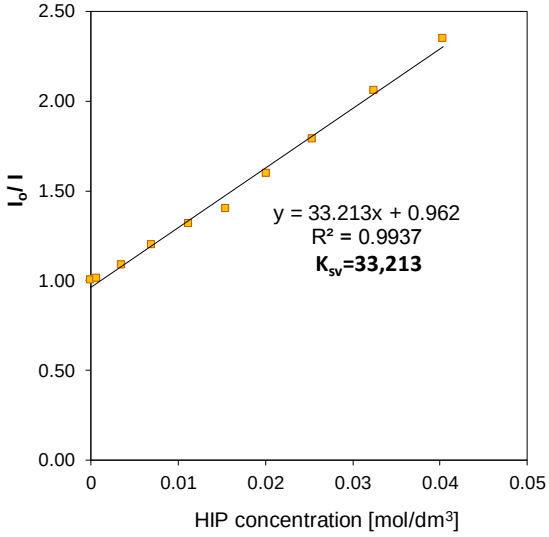

Figure S.50. Stern-Volmer treatment for the

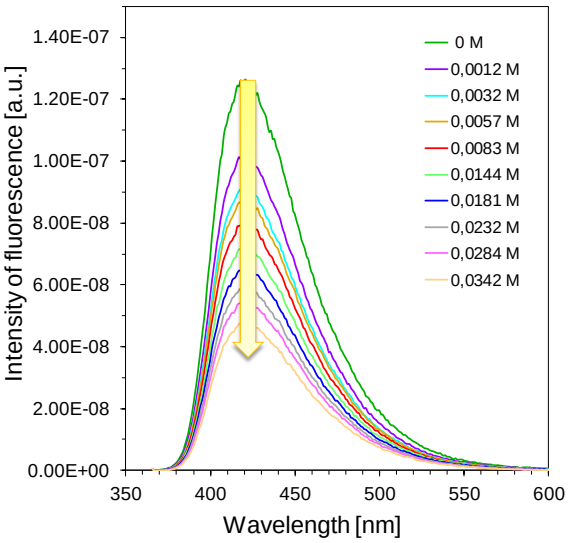

Figure S.51. Fluorescence quenching of S6.

S5/HIP fluorescence quenching.

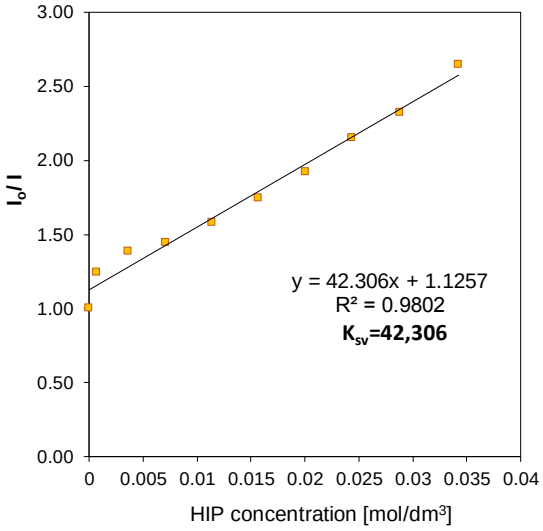

Figure S.52. Stern-Volmer treatment for the S6/HIP fluorescence quenching.

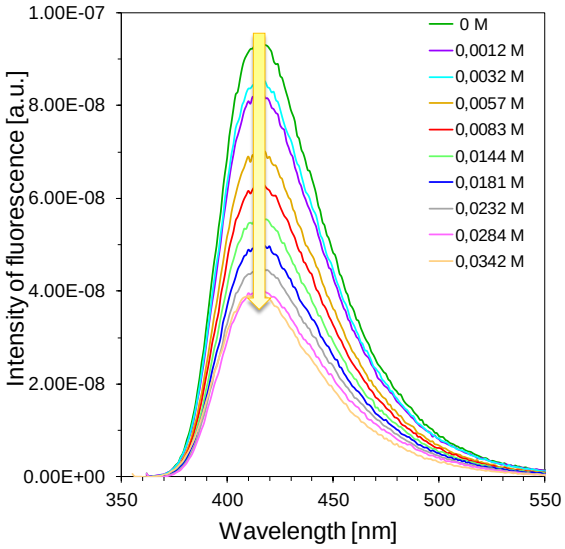

Figure S.53. Fluorescence quenching of S7.

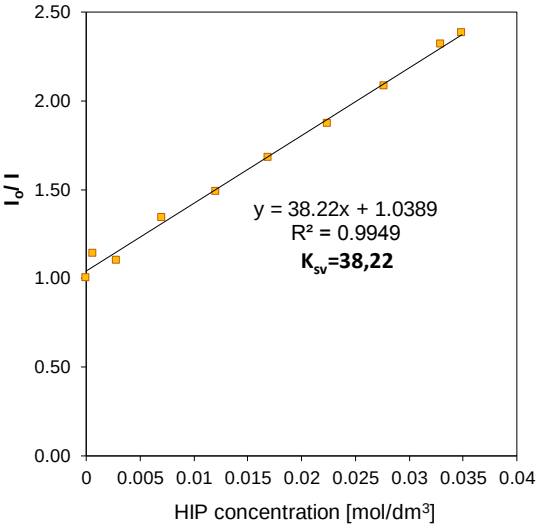

Figure S.54. Stern-Volmer treatment for the S7/HIP fluorescence quenching.

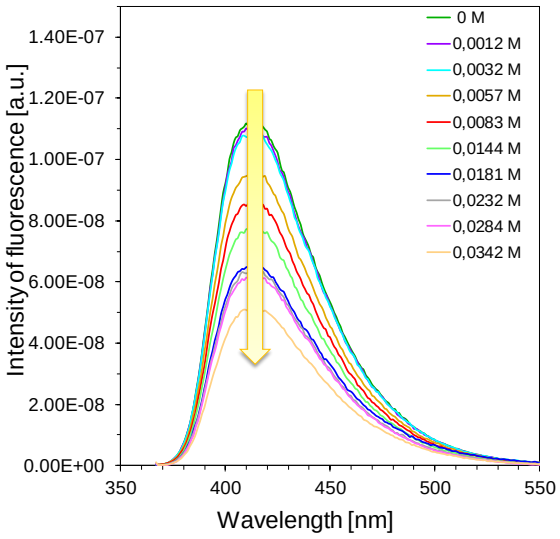

Figure S.55. Fluorescence quenching of S8.

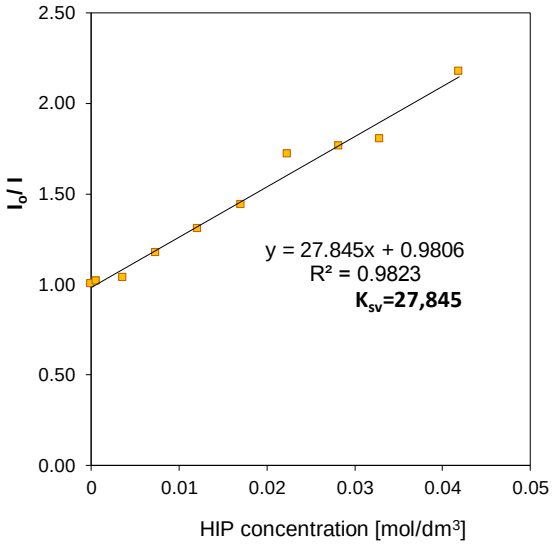

Figure S.56. Stern-Volmer treatment for the S8/HIP fluorescence quenching.

Fluorescence quenching with EDB of investigated 2-amino-4,6-diphenylpyridine-3-carbonitrile derivatives together with Stern-Volmer correlation

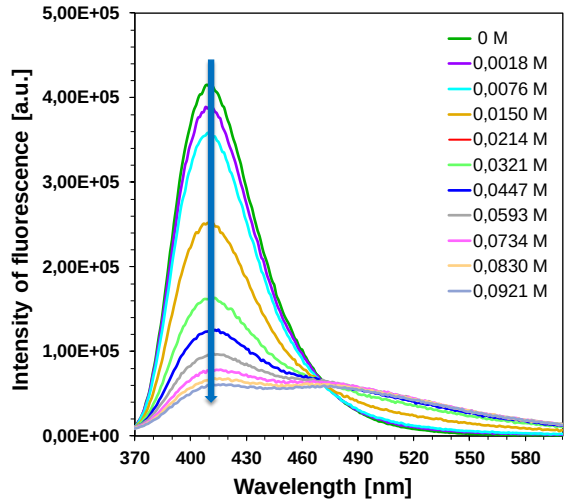

Figure S.57. Fluorescence quenching of S1 with EDB.

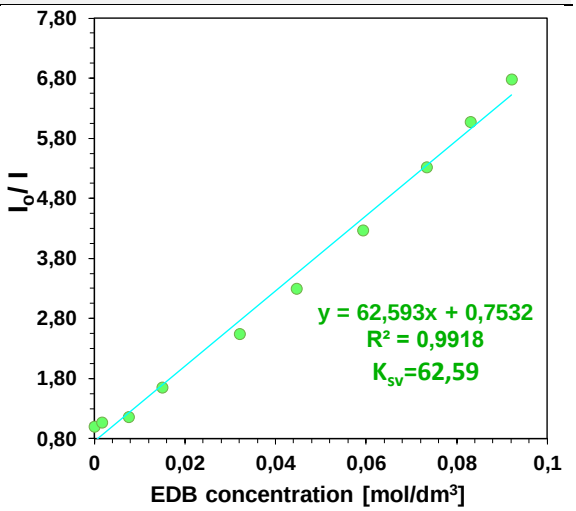

Figure S.58. Stern-Volmer treatment for the S1/EDB fluorescence quenching.

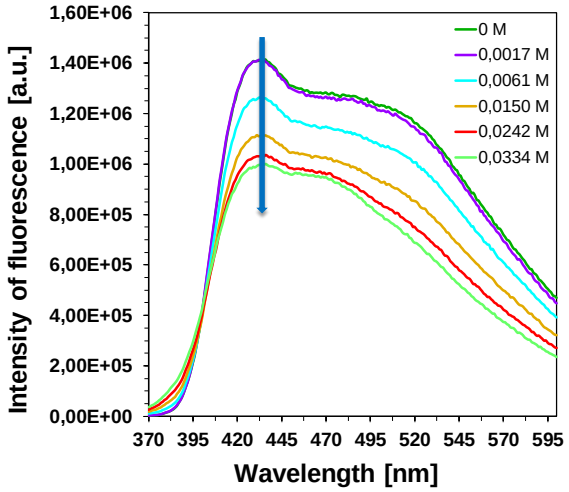

Figure S.59. Fluorescence quenching of S2 with EDB.

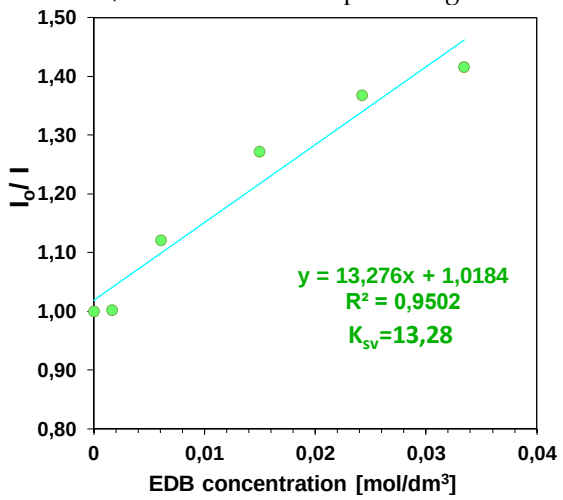

Figure S.60. Stern-Volmer treatment for the S2/EDB fluorescence quenching.

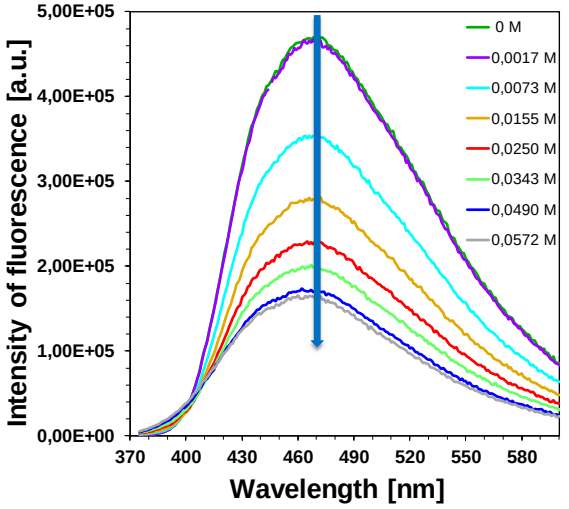

Figure S.61. Fluorescence quenching of S3 with

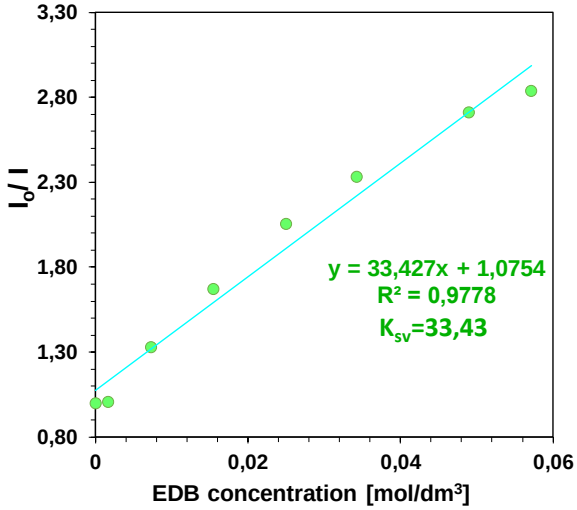

Figure S.62. Stern-Volmer treatment for the

EDB.

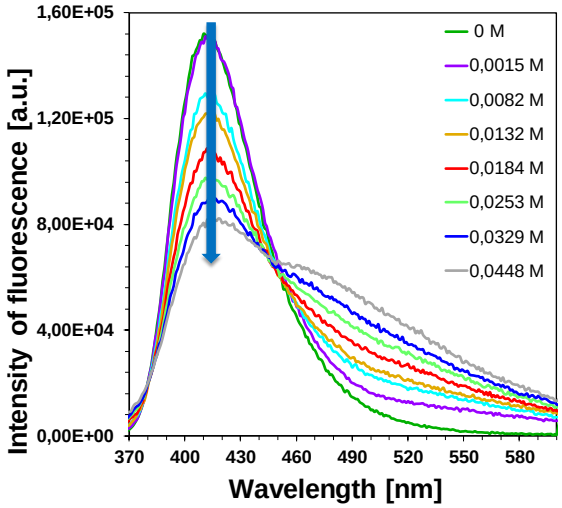

Figure S.63. Fluorescence quenching of S4with EDB.

S3/EDB fluorescence quenching.

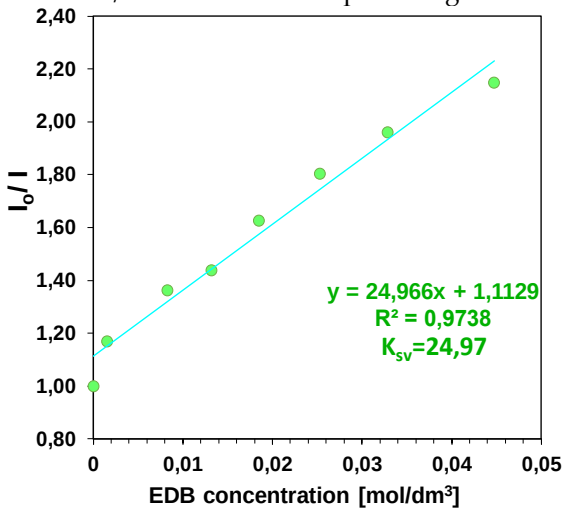

Figure S.64. Stern-Volmer treatment for the S4/EDB fluorescence quenching.

EDB.

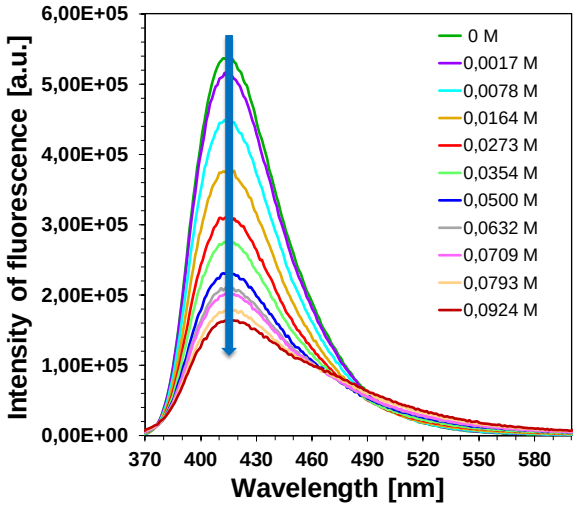

Figure S.65. Fluorescence quenching of S5 with EDB.

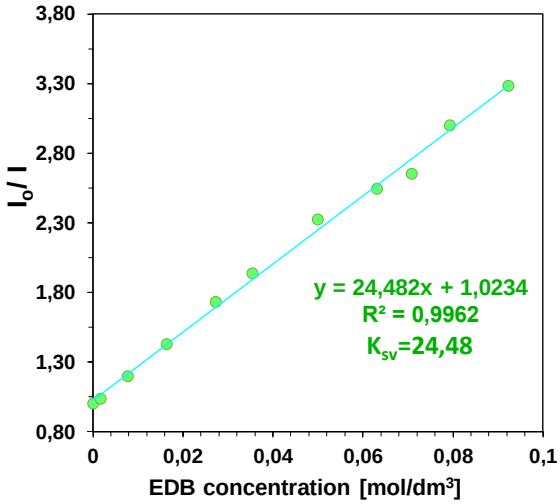

Figure S.66. Stern-Volmer treatment for the S5/EDB fluorescence quenching.

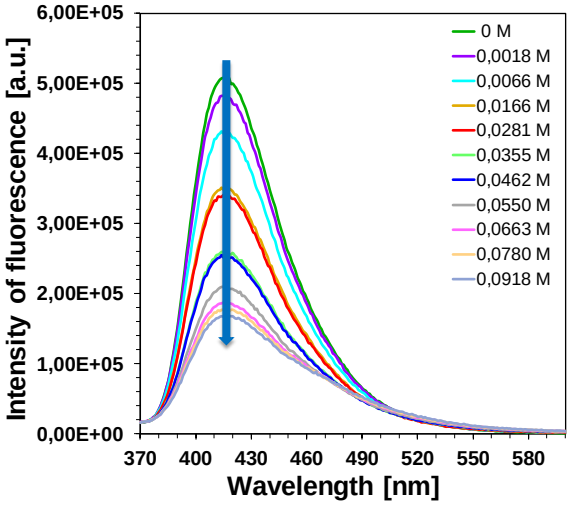

Figure S.67. Fluorescence quenching of S6 with EDB.

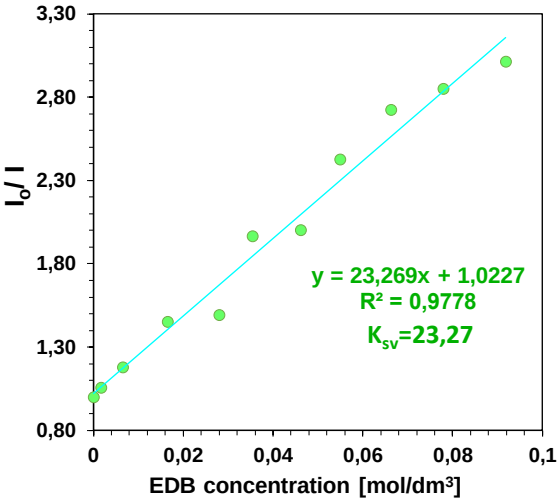

Figure S.68. Stern-Volmer treatment for the S6/EDB fluorescence quenching.

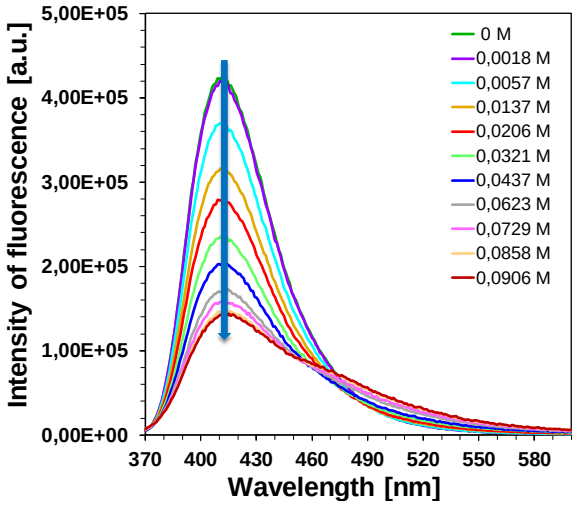

Figure S.69. Fluorescence quenching of S7 with EDB.

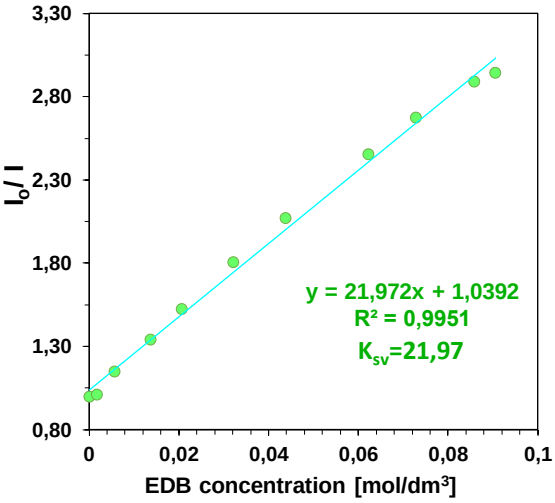

Figure S.70. Stern-Volmer treatment for the S7/EDB fluorescence quenching.

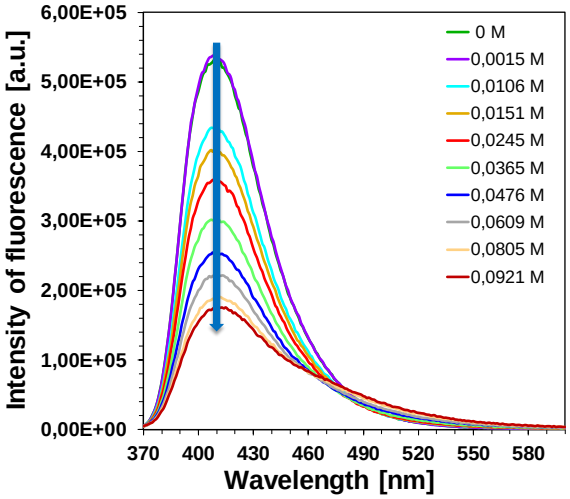

Figure S.71. Fluorescence quenching of S8 with EDB.

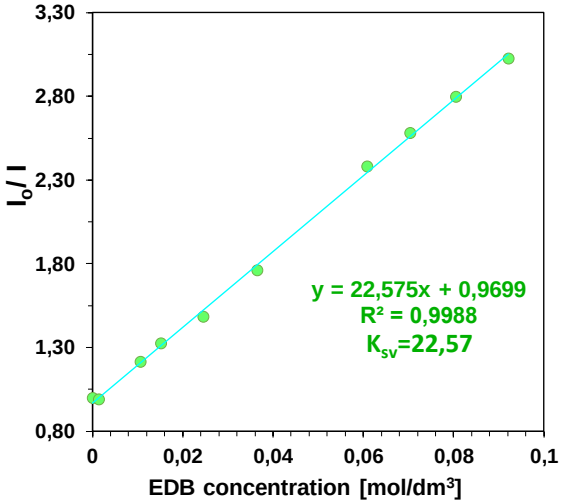

Figure S.72. Stern-Volmer treatment for the S8/EDB fluorescence quenching.

Steady state photolysis upon exposure with LED @365nm for of investigated 2-amino-4,6-diphenylpyridine-3-carbonitrile derivatives in acetonitrile

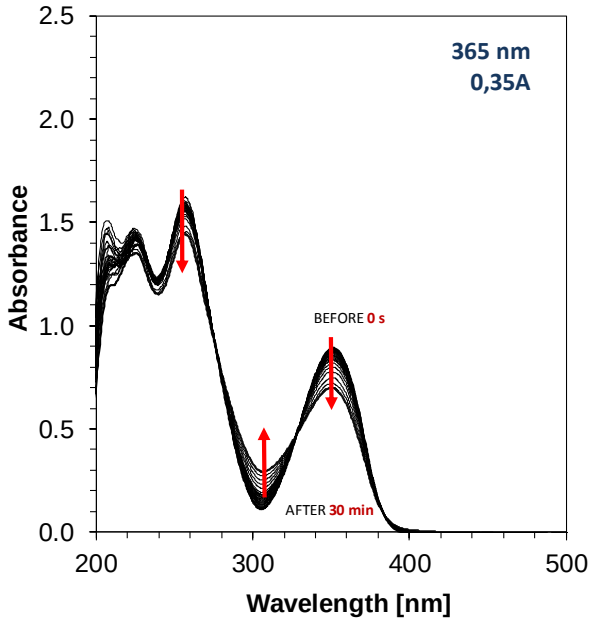

Figure S.73. Photolysis of S1 in ACN under 365nm (126mW/cm²).

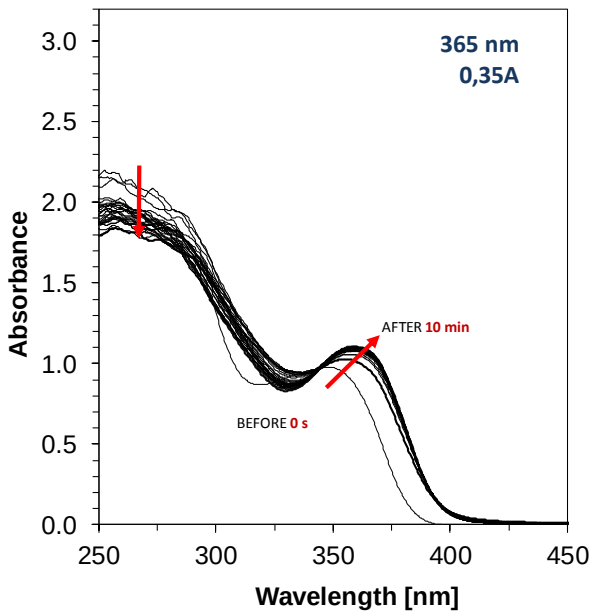

Figure S.74. Photolysis of S1 + HIP (concentration: $2.01 \cdot 10^{-3}$ [mol/dm³]) in ACN under 365nm (126mW/cm²).

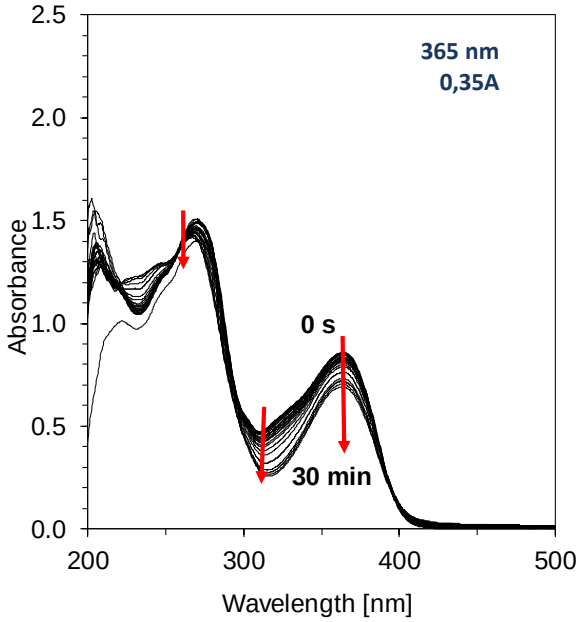

Figure S.75. Photolysis of S2 in ACN under 365nm (126mW/cm²).

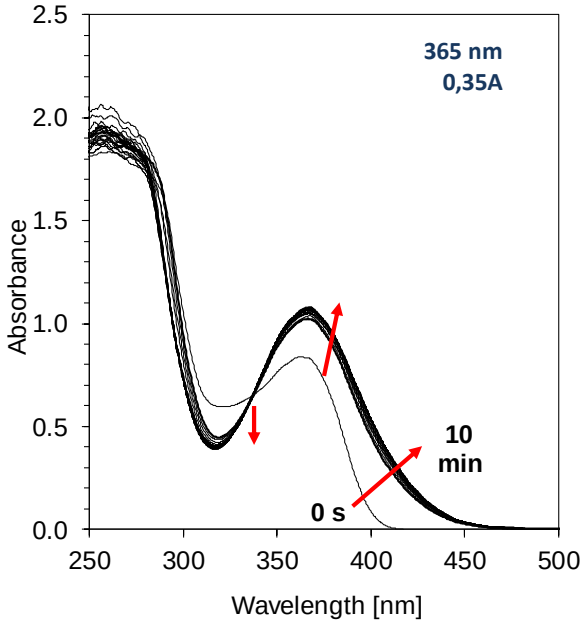

Figure S.76. Photolysis of S2 + HIP (concentration: $2.01 \cdot 10^{-3}$ [mol/dm³]) in ACN under 365nm (126mW/cm²).

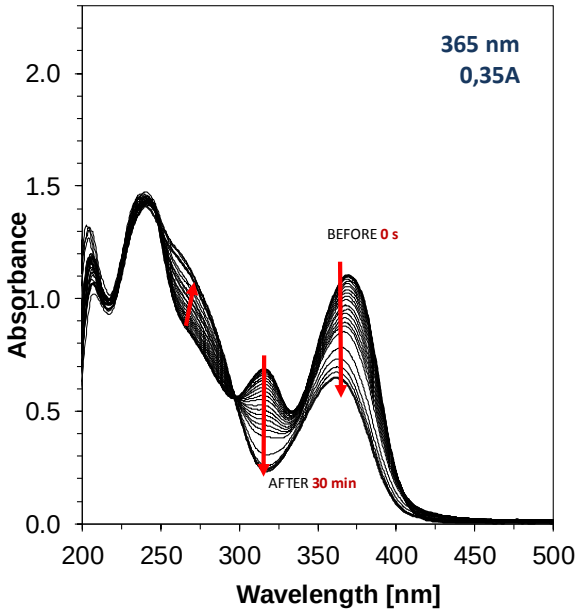

Figure S.77. Photolysis of S3 in ACN under 365nm (126mW/cm²).

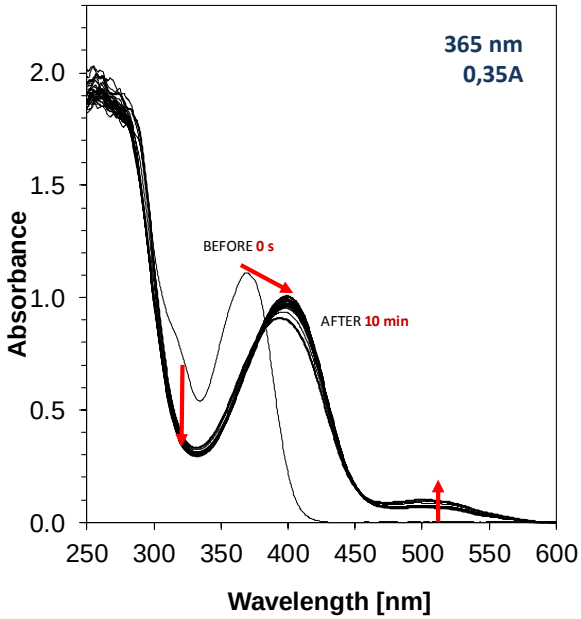

Figure S.78. Photolysis of S3 + HIP (concentration: $2.01 \cdot 10^{-3}$ [mol/dm³]) in ACN under 365nm (126mW/cm²).

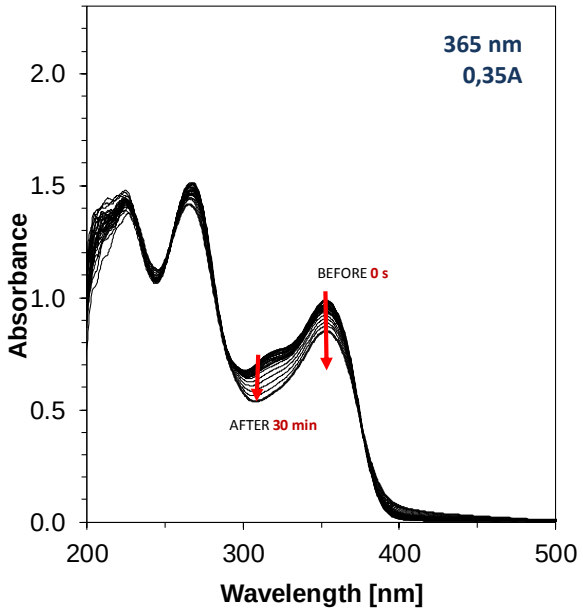

Figure S.79. Photolysis of S4 in ACN under 365nm (126mW/cm²).

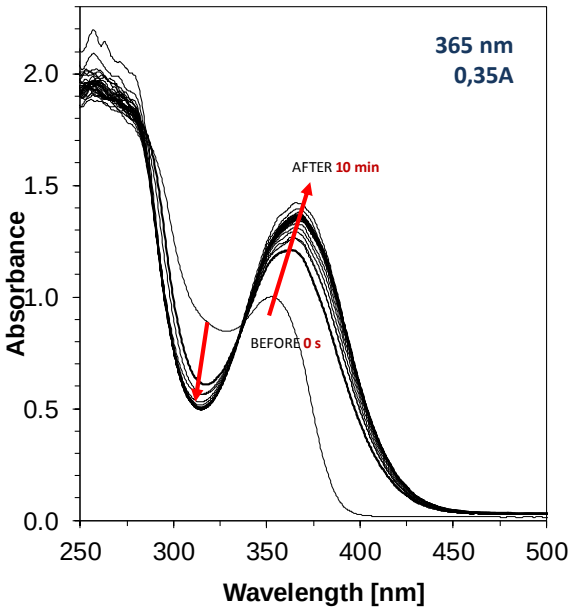

Figure S.80. Photolysis of S4 + HIP (concentration: $2.01 \cdot 10^{-3}$ [mol/dm³]) in ACN under 365nm (126mW/cm²).

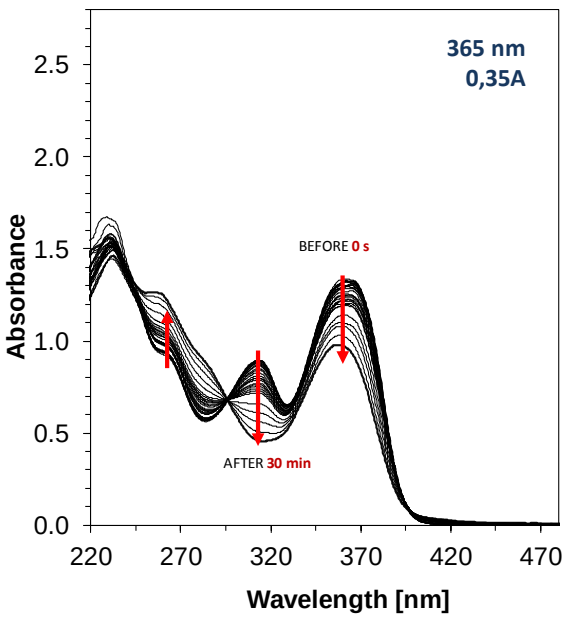

Figure S.81. Photolysis of S5 in ACN under 365nm (126mW/cm²).

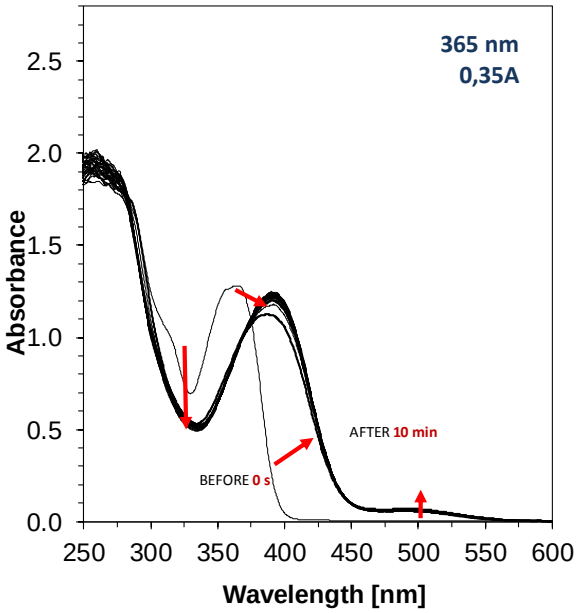

Figure S.82. Photolysis of S5 + HIP (concentration: $2.01 \cdot 10^{-3}$ [mol/dm³]) in ACN under 365nm (126mW/cm²).

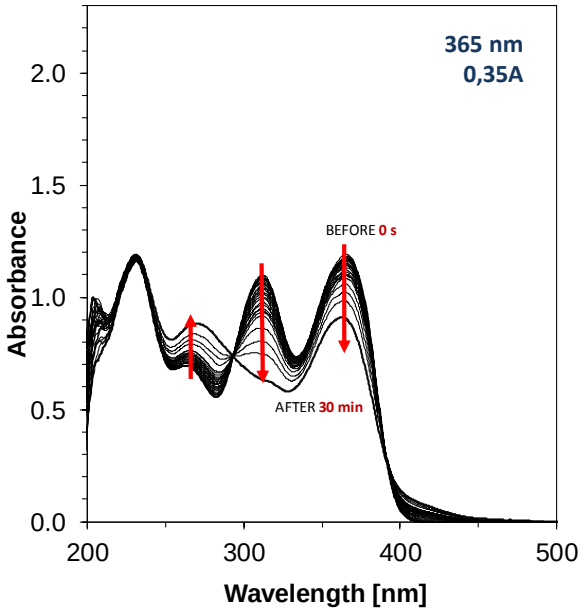

Figure S.83. Photolysis of S6 in ACN under 365nm (126mW/cm²).

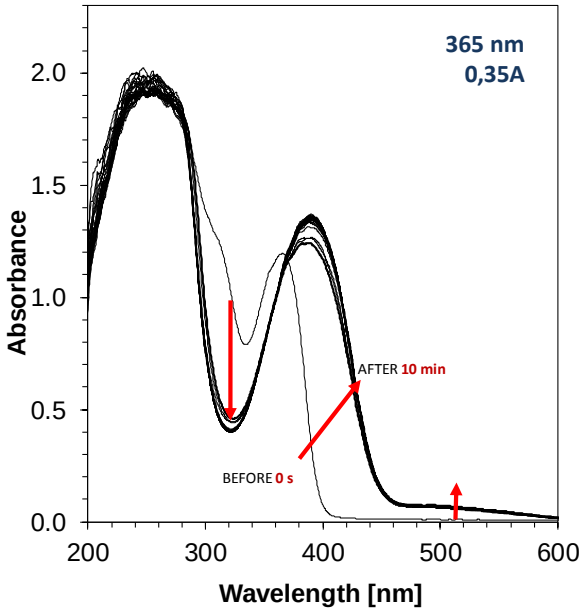

Figure S.84. Photolysis of S6 + HIP (concentration: $2.01 \cdot 10^{-3}$ [mol/dm³]) in ACN under 365nm (126mW/cm²).

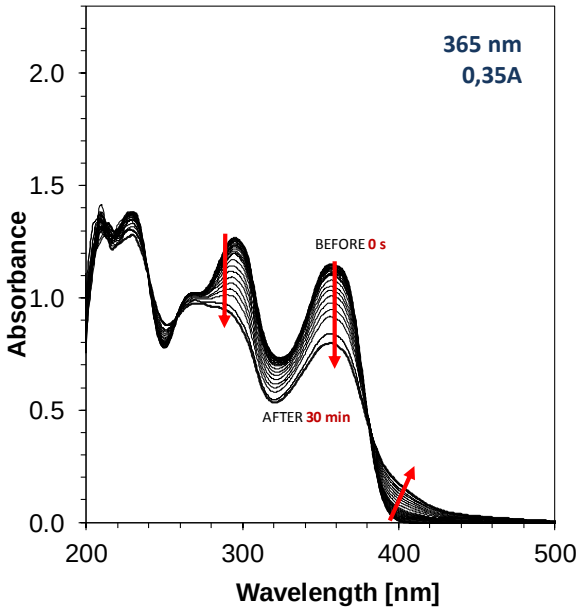

Figure S.85. Photolysis of S7 in ACN under 365nm (126mW/cm²).

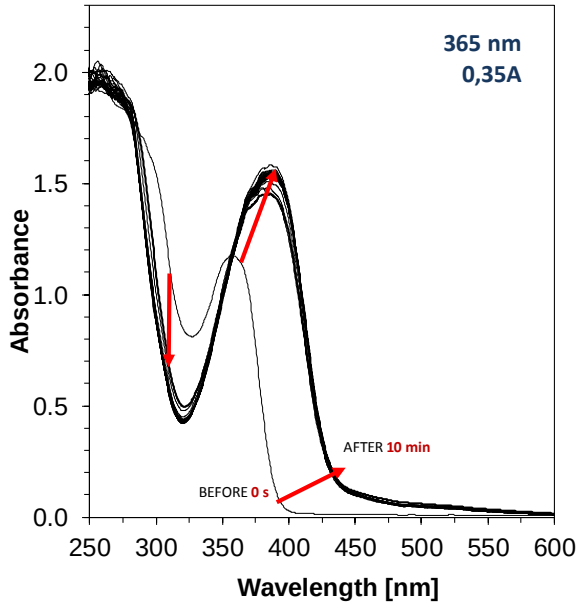

Figure S.86. Photolysis of S7 + HIP (concentration: $2.01 \cdot 10^{-3}$ [mol/dm³]) in ACN under 365nm (126mW/cm²).

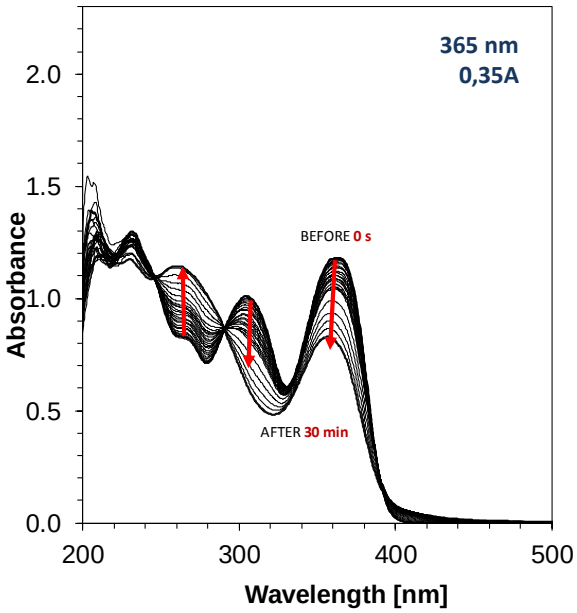

Figure S.87. Photolysis of S8 in ACN under 365nm (126mW/cm²).

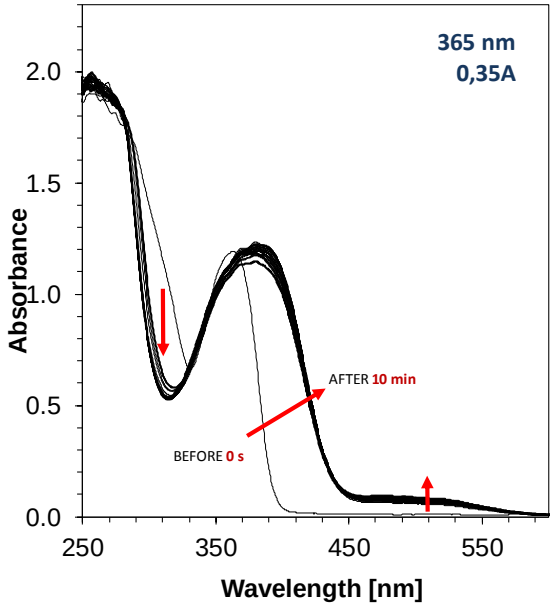

Figure S.88. Photolysis of S8 + + HIP (concentration: $2.01 \cdot 10^{-3}$ [mol/dm³]) in ACN under 365nm (126mW/cm²).

Steady state photolysis upon exposure with LED @405nm for of investigated 2-amino-4,6-diphenylpyridine-3-carbonitrile derivatives in acetonitrile

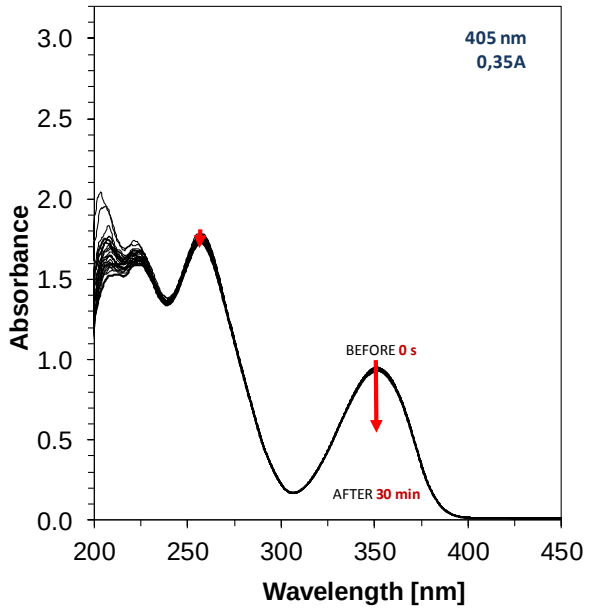

Figure S.89. Photolysis of S1 in ACN under 405nm (455mW/cm²).

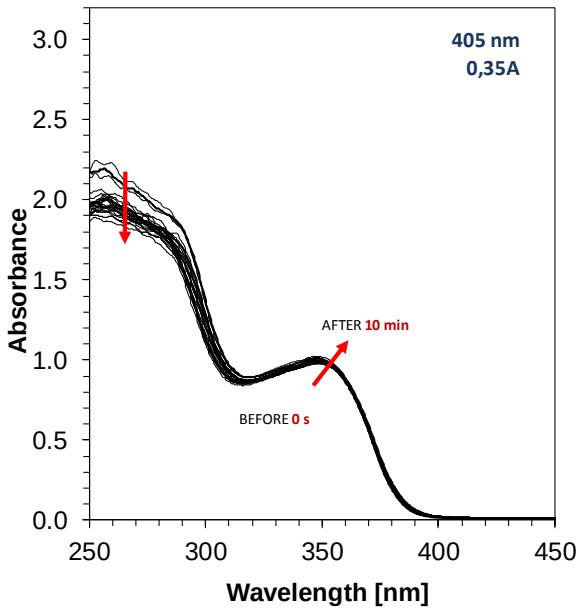

Figure S.90. Photolysis of S1 + HIP (concentration: $2.01 \cdot 10^{-3}$ [mol/dm³]) in ACN under 405nm (455mW/cm²).

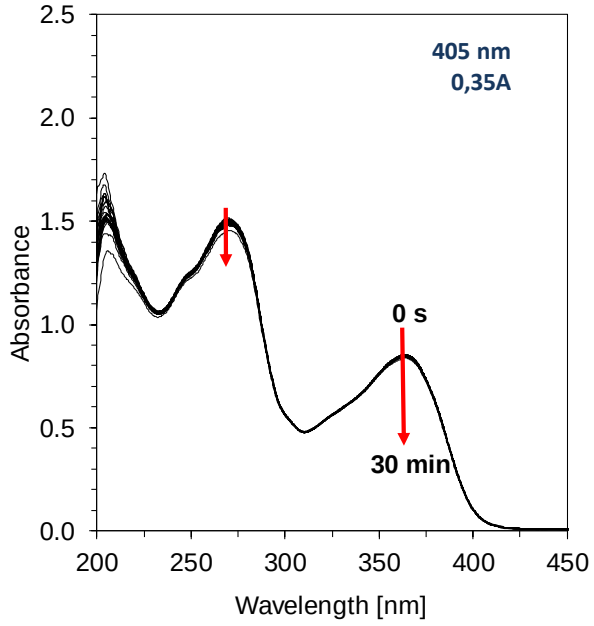

Figure S.91. Photolysis of S2 in ACN under 405nm (455mW/cm²).

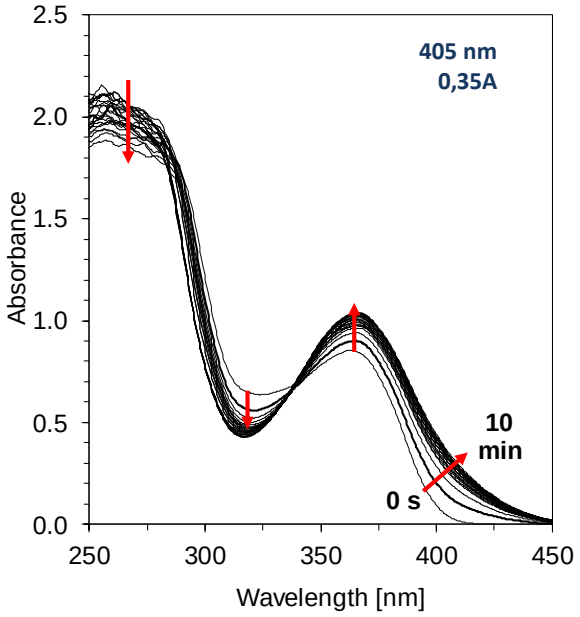

Figure S.92. Photolysis of S2 + HIP (concentration: $2.01 \cdot 10^{-3}$ [mol/dm³]) in ACN under 405nm (455mW/cm²).

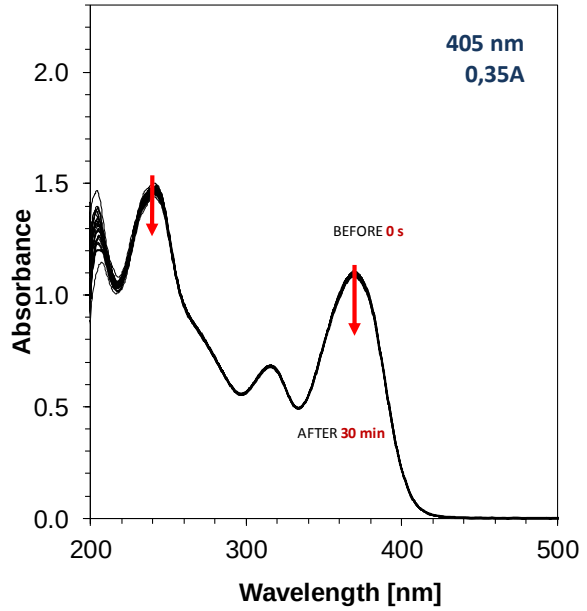

Figure S.93. Photolysis of S3 in ACN under 405nm (455mW/cm²).

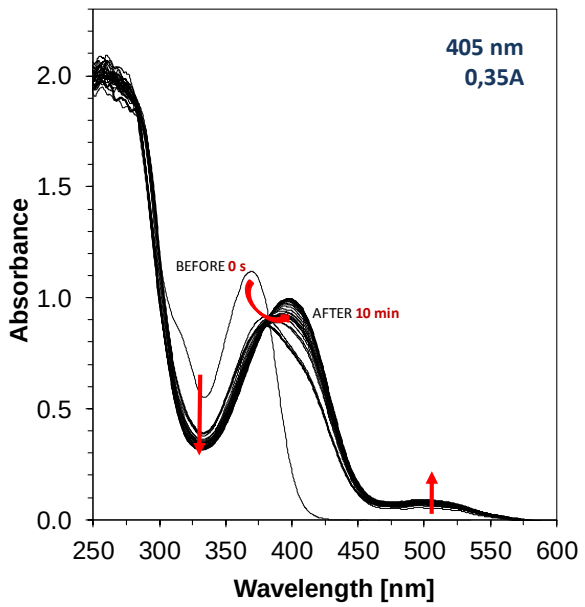

Figure S.94. Photolysis of S3 + HIP (concentration: $2.01 \cdot 10^{-3}$ [mol/dm³]) in ACN under 405nm (455mW/cm²).

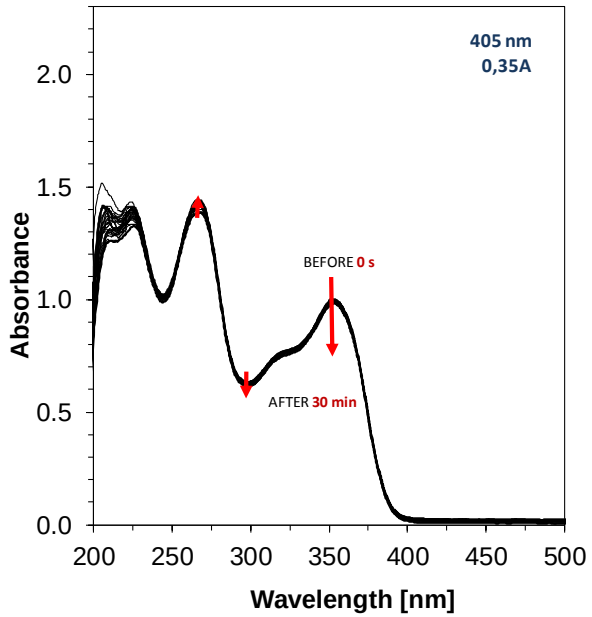

Figure S.95. Photolysis of S4 in ACN under 405nm (455mW/cm²).

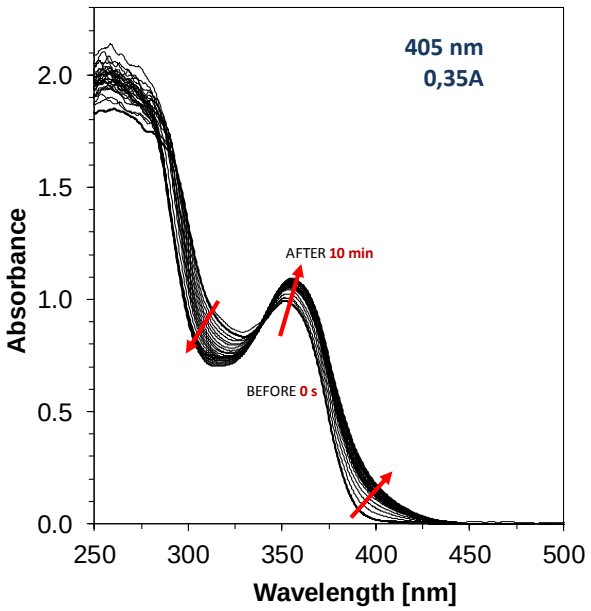

Figure S.96. Photolysis of S4 + HIP (concentration: $2.01 \cdot 10^{-3}$ [mol/dm³]) in ACN under 405nm (455mW/cm²).

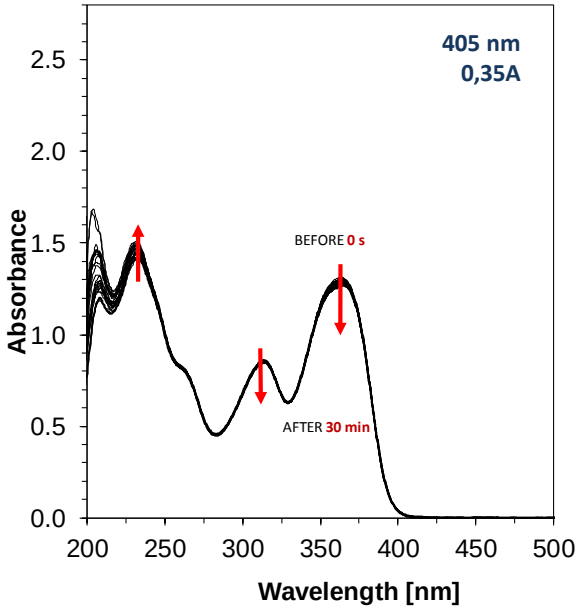

Figure S.97. Photolysis of S5 in ACN under 405nm (455mW/cm²).

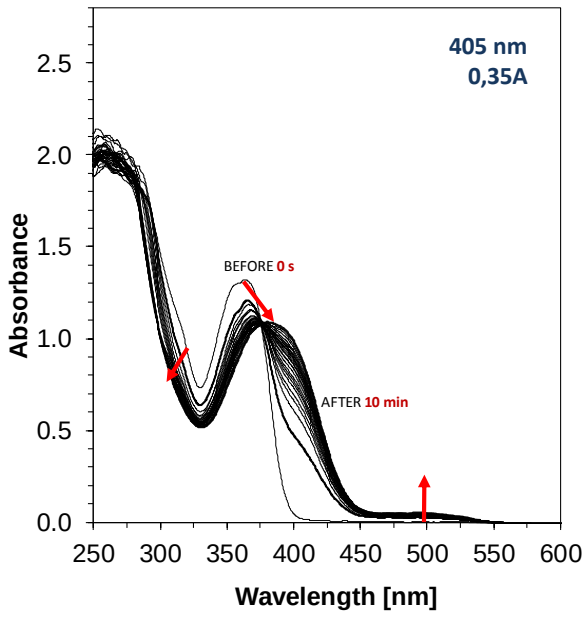

Figure S.98. Photolysis of S5 + HIP (concentration: $2.01 \cdot 10^{-3}$ [mol/dm³]) in ACN under 405nm (455mW/cm²).

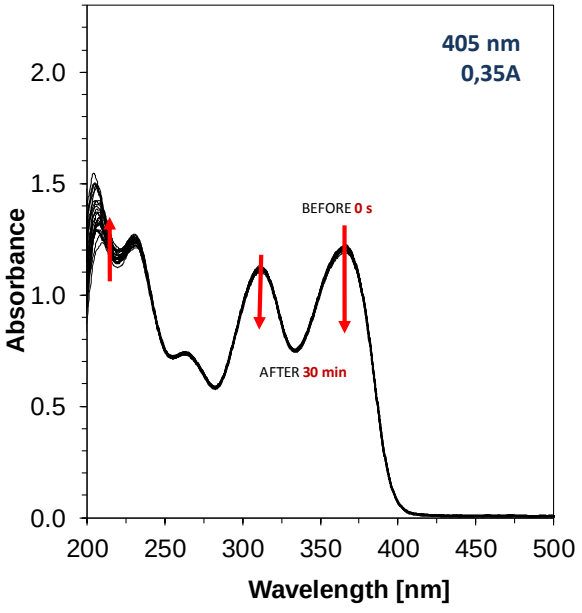

Figure S.99. Photolysis of S6 in ACN under 405nm (455mW/cm²).

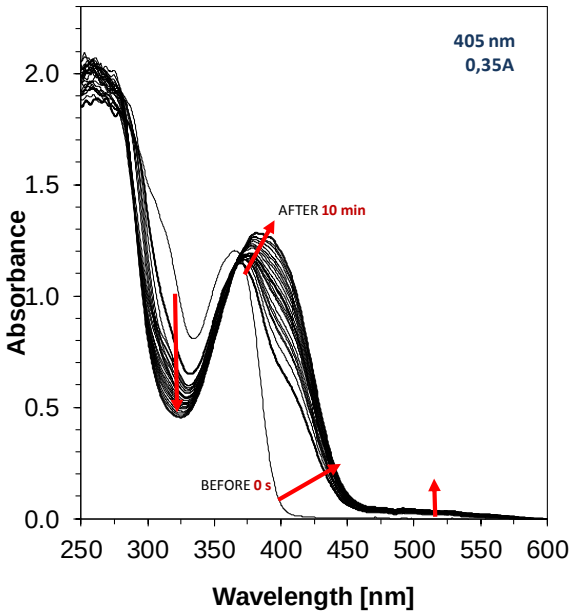

Figure S.100. Photolysis of S6 + HIP (concentration: $2.01 \cdot 10^{-3}$ [mol/dm³]) in ACN under 405nm (455mW/cm²).

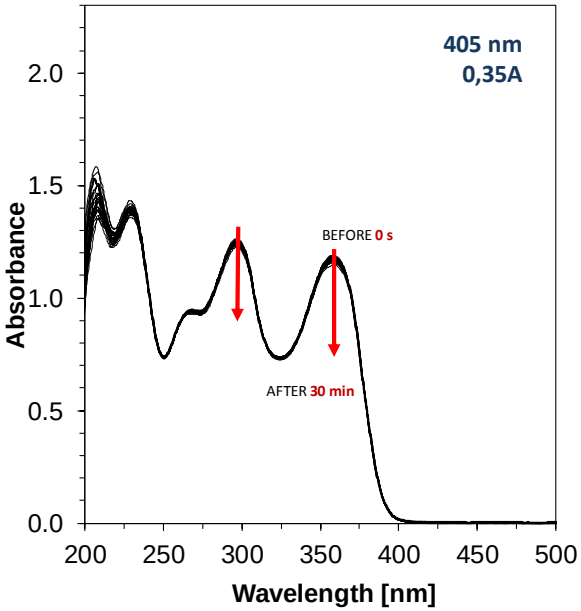

Figure S.101. Photolysis of S7 in ACN under 405nm (455mW/cm²).

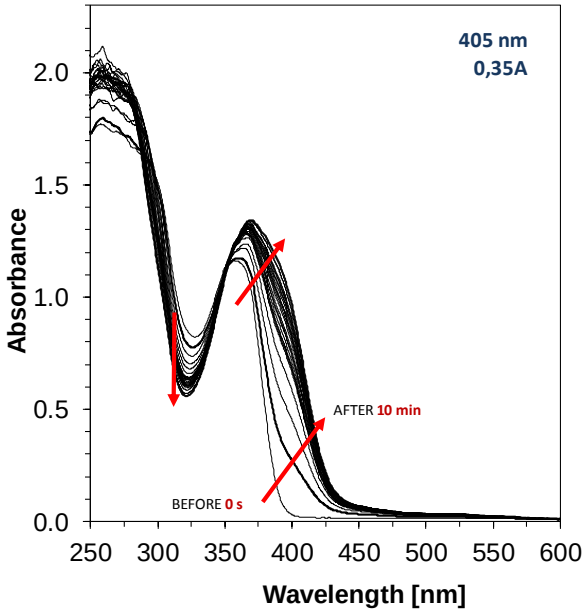

Figure S.102. Photolysis of S7 + HIP (concentration: $2.01 \cdot 10^{-3}$ [mol/dm³]) in ACN under 405nm (455mW/cm²).

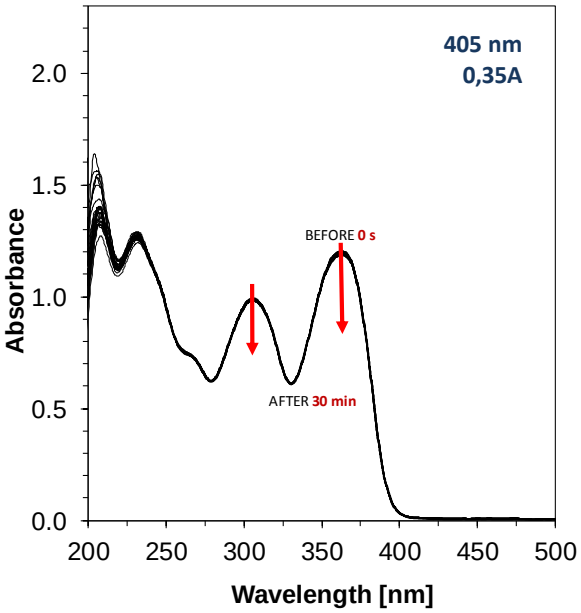

Figure S.103. Photolysis of S8 in ACN under 405nm (455mW/cm²).

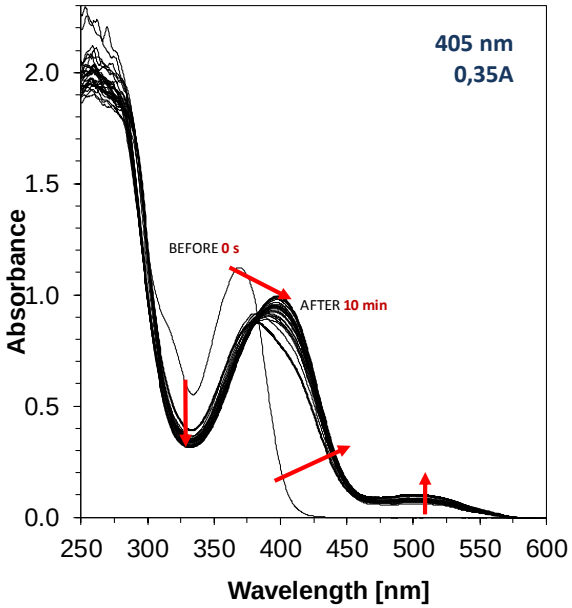

Figure S.104. Photolysis of S8 + HIP (concentration: $2.01 \cdot 10^{-3}$ [mol/dm³]) in ACN under 405nm (455mW/cm²).

Steady state photolysis upon exposure with LED @405nm for of investigated 2-amino-4,6-diphenylpyridine-3-carbonitrile derivatives and EDB in acetonitrile

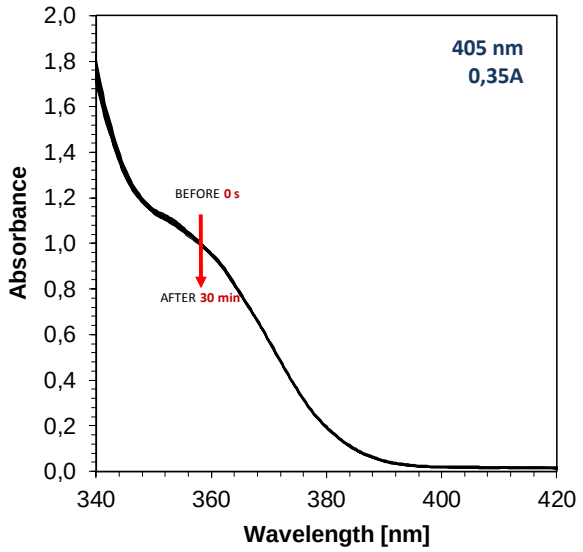

Figure S.105. Photolysis of S1 + EDB (concentration: $4.436 \cdot 10^{-3}$ [mol/dm^3]) in ACN under 405nm (455mW/cm^2).

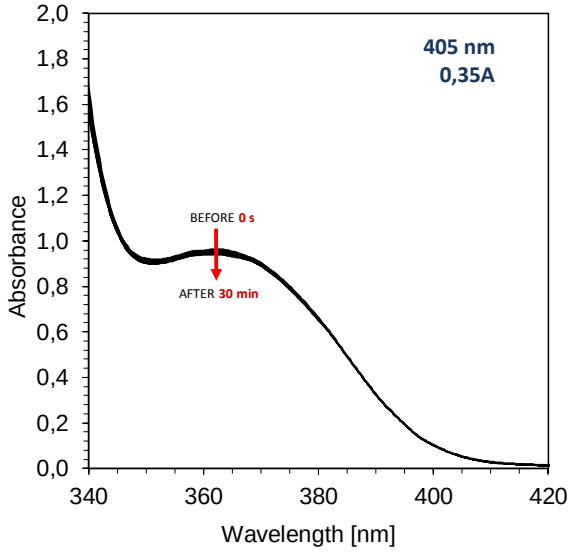

Figure S.106. Photolysis of S2 + EDB (concentration: $4.436 \cdot 10^{-3}$ [mol/dm^3]) in ACN under 405nm (455mW/cm^2).

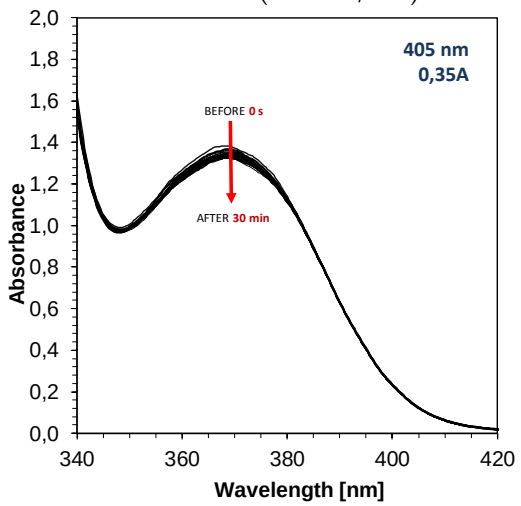

Figure S.107 Photolysis of S3 + EDB (concentration: $4.436 \cdot 10^{-3}$ [mol/dm^3]) in ACN under 405nm (455mW/cm^2).

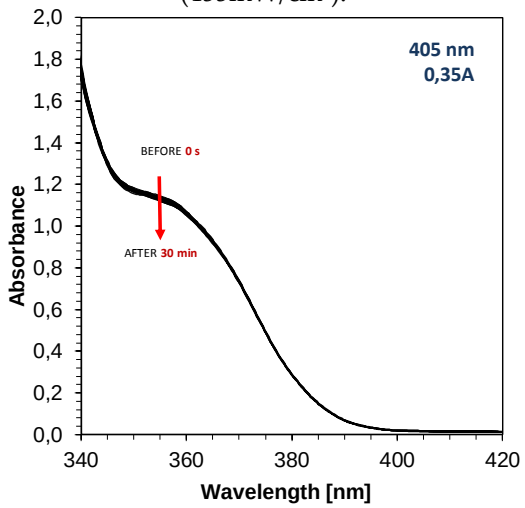

Figure S.108. Photolysis of S4+ EDB (concentration: $4.436 \cdot 10^{-3}$ [mol/dm^3]) in ACN under 405nm (455mW/cm^2).

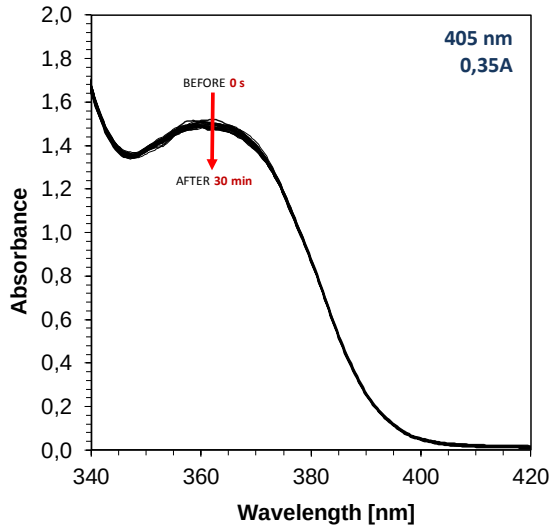

Figure S.109. Photolysis of S5 + EDB (concentration: $4.436 \cdot 10^{-3}$ [mol/dm^3]) in ACN under 405nm (455mW/cm^2).

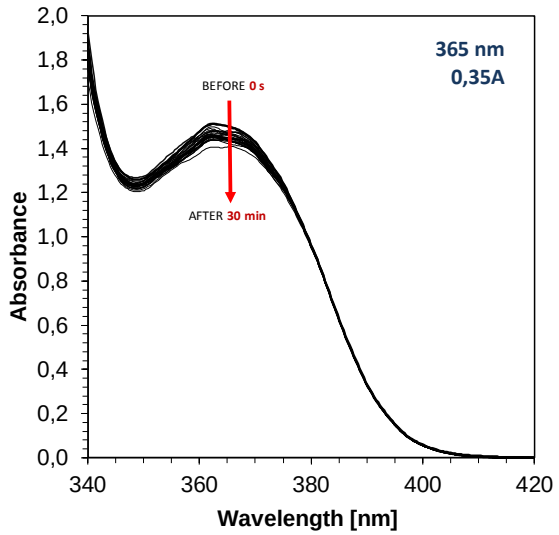

Figure S.110. Photolysis of S6 + EDB (concentration: $4.436 \cdot 10^{-3}$ [mol/dm^3]) in ACN under 405nm (455mW/cm^2).

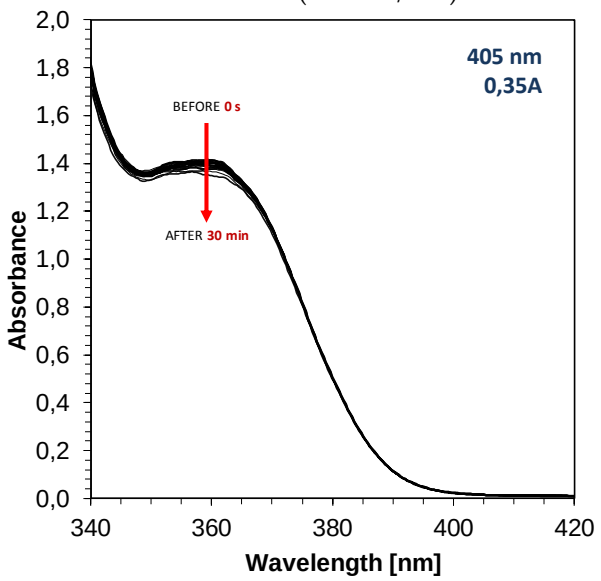

Figure S.111. Photolysis of S7 + EDB (concentration: $4.436 \cdot 10^{-3}$ [mol/dm^3]) in ACN under 405nm (455mW/cm^2).

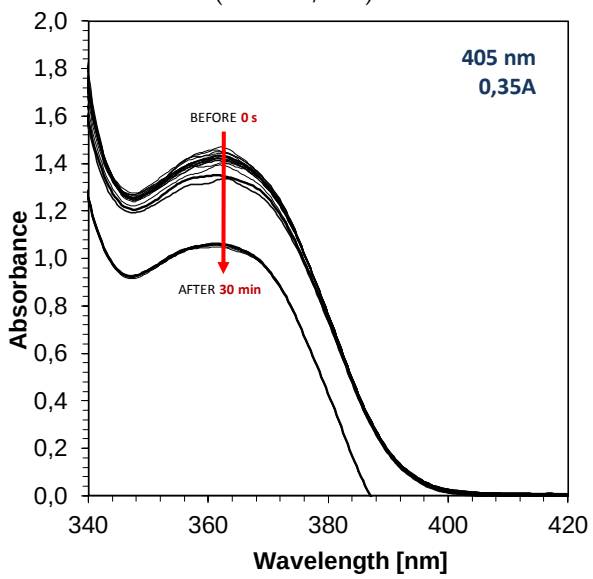

Figure S.112. Photolysis of S8 + EDB (concentration: $4.436 \cdot 10^{-3}$ [mol/dm^3]) in ACN under 405nm (455mW/cm^2).

References:

[1] S. Kambe, K. Saito, A. Sakurai, H. Midorikawa, A simple method for the preparation of 2-amino-4-aryl-3-cyanopyridines by the condensation of malononitrile with aromatic aldehydes and alkyl ketones in the presence of ammonium acetate, Synth. 1980 (1980) 366–368. doi:10.1055/s-1980-29021.

[2] J. Ortyl, P. Fiedor, A. Chachaj-Brekiesz, M. Pilch, E. Hola, M. Galek, The Applicability of 2-amino-4,6-diphenyl-pyridine-3-carbonitrile Sensors for Monitoring Different Types of Photopolymerization Processes and Acceleration of Cationic and Free-Radical Photopolymerization Under Near UV Light. Sensors 2019, 19, 1668-1690. doi:10.3390/s19071668.